DOI:10.14753/SE.2018.2148

THE ROLE OF NEURON-MICROGLIA FRACTALKINE SIGNALING IN ORGANIZATION OF RESPONSES TO ACUTE AND CHRONIC STRESSORS

PhD thesis

Zsuzsanna Winkler

János Szentágothai Doctoral School of Neuroscience

Semmelweis University

Supervisor: Krisztina Kovács, D.Sc

Official reviewers: Árpád Dobolyi, D.Sc
István Ábrahám, D.Sc

Head of the Final Examination Committee: Károly Rácz, MD, D.Sc

Members of the Final Examination Committee: Imre Kalló, Ph.D
Anna Földes, Ph.D

Budapest

2017

DOI:10.14753/SE.2018.2148

Table of Contents

DOI:10.14753/SE.2018.2148

DOI:10.14753/SE.2018.2148

DOI:10.14753/SE.2018.2148

1. The list of Abbreviation

2-DG	2-deoxy-glucose
ACTH	adrenocorticotrop hormone
AgRP	agouti-related peptid
ARC	hypothalamic arcuate nucleus
C1	catecholaminergic group of cells in the basolateral medulla
CART	cocaine- and amphetamine-regulated transcript
CNS	central nervous system
CORT	corticosterone
CRH	corticotropin-releasing hormone
CSF1R	colony stimulating factor 1 receptor
CVS	chronic variable stress
CX_3CR1	fractalkine receptor
$CX_3CR1^{-/-}$ mice	fractalkine receptor deficient mice
DAMPS	danger-associated molecular patterns
dBNST	bed nucleus of the stria terminalis
EPM	elevated plus maze test
FFAs	free fatty acids
FST	forced swim test
GE neurons	glucose excited
GI neurons	glucose inhibited
GLUT5	glucose transporter 5
GR	glucocorticoid receptor
HAAF	hypoglycemia associated autonomic failure
HFD	high-fat diet
HMGB1	high-mobility group box 1
HPA axis	hypothalamo–pituitary–adrenocortical axis
Hsp72	heat-shock protein 72

Iba1	ionized calcium-binding adaptor molecule 1
icv.	intracerebroventricular
IEG	immediate early gene
IGF-1	insulin-like growth factor 1
IL-1	interleukin-1
ip.	intraperitoneal
ir.	immunoreactivity
IRS-1, IRS-2	insulin receptor substrates 1, 2
KATP channel	ATP-sensitive potassium channel
LPS	lipopolysaccharide
MBH	mediobasal hypothalamus
MCT1, MCT2	monocarboxylate transporters 1,2
MePO	median pre-optic nucleus
mPFC	medial prefrontal cortex
MR	mineralocorticoid receptors
MS	maternal separation
NE	norepinephrine
NF-κB	nuclear factor kappa-light-chain-enhancer of activated B cells
NLRP3	NACHT, LRR and PYD domains-containing protein 3
NPY	neuropeptide Y
NTS	nucleus of the solitary tract
OGD	oxygen glucose deprivation
OVLT	vascular organ of lamina terminalis
P2X7	P2X purinoceptor 7
PAG	periaqueductal gray
PAMPS	pathogen activated molecular patterns
PB	parabrachial nucleus
pCREB	phosphorylation of cyclic AMP response element binding
PKA	protein kinase A

DOI:10.14753/SE.2018.2148

PLX5622	Plexxikon 5622
POMC	proopimelanocortin
PVN	hypothalamic paraventricular nucleus
RT-qPCR	Real-time quantitative PCR
SEM	standard error of the mean
SFO	subfornical organ
siRNA	silencing ribonucleic acid
TH	tyrosine hydroxylase
TLRs	toll-like receptors
TST	tail suspension test

DOI:10.14753/SE.2018.2148

2. Introduction

2.1. The stress concept/ Homeostasis and allostasis

All living organisms strive to maintain homeostasis, a dynamic equilibrium of crucial internal parameters. Walter Cannon was the first who defined the term "homeostasis", as "coordinated physiological processes which maintain most of the steady states in the organism" [1]. Hans Selye defined "stress" as a nonspecific response of the body, the "stress syndrome" with the same pathological triad (adrenal enlargement, thymus involution, gastrointestinal ulceration) evoked by diverse kind of stressors (bacterial infection, toxins, physical stimuli) [2]. Selye also introduced the phrase "general adaptation syndrome", which consists of three successive phases: alarm reaction (mobilizing resources), stage of resistance (coping with stressor), stage of exhaustion [3].

The first definition of allostasis was introduced by Sterling and Eyer, which literally means "achieving stability through change" [4]. Stressors trigger physiological and behavioral responses that are aimed at reinstating a new balance, help the organism to cope with the situation. Stress response is manifested as rapid activation of the sympathetic nervous system and hypothalamo-pituitary-adrenocortical (HPA) axis, but includes changes in many other central and peripheral functions including autonomic arousal, metabolism, immune and hormonal regulation, cognition, emotion, memory and behavior. The coping is effective, if the stress response is rapidly activated and efficiently terminated [5]. The processes that underlie the stress response have been collectively termed "allostasis". If the stress response is inadequate or excessive and prolonged, the cost of restoring homeostasis might become too high, and can lead to maladaptation (cardiovascular, gastrointestinal, metabolic, immunological dysfunction and mood disorders). The term, allostatic load was proposed by McEwen [6] and is the "price" of the adaptation during lifespan. There are four major conditions that lead to allostatic load:

- repeated hits from multiple stressors
- lack of habituation to the recurrence of the same stressor
- prolonged response: not turning off the response when it is no longer needed
- inadequate response: for example inadequate secretion of glucocorticoids

In terms of duration, stressors may be classified into two main categories: acute or chronic, prolonged exposure [7]. Acute stressors induce adaptive physiological and behavioral responses that are essential to reinstate homeostatic balance. Acute stress mobilizes energy reserves, sensitizes immune cells to provide tools for coping and for preparation for future exposure to additional, predictable or unpredictable challenges. In the stress response, fast-acting agents (such as catecholamines, neuropeptides, non-genomic glucocorticoid action) and slower, gene-mediated corticosteroid effects contribute to an adequate response to the stressor, which leads to enhanced vigilance, alertness and focused attention. At systems level, increase of gluconeogenesis, glycogenolysis, proteolysis or lipolysis provide energy supply to "crucial" organs.

2.2. The hypothalamo-pituitary-adrenocortical (HPA) axis

The neuroendocrine stress response can be viewed as a reflex regulation, where corticotropin-releasing hormone (CRH) and vasopressin (AVP)-synthesizing neurons in the parvocellar part of the hypothalamic paraventricular nucleus (PVN) are in the reflex centrum. These neuropeptides are secreted into the portal vessel system and stimulate adrenocorticotropin (ACTH) from the pituitary. ACTH increases adrenal cortical secretion of cortisol (in human), and corticosterone (in rodents). Corticosteroids are bound to nuclear mineralocorticoid (MR) and glucocorticoid (GR) receptors. MR is implicated in the appraisal process and the early-phase of the stress response. GR is activated by higher amounts of corticosteroids, terminate stress reactions, mobilize energy resources and facilitate recovery [8].

2.3. Afferent inputs to CRH neurons in the paraventricular nucleus (PVN)

Several afferent inputs trigger directly the stress-related CRH neurons in the PVN. These include pathways arising from neuron groups associated with most major sensory systems (**Fig.1.**) [9]. Viscerosensory and somatosensory inputs are transduced by the ascending (catecholaminergic) pathway originating in the nucleus of the solitary tract and associated structures in the ventrolateral medulla [10] [11]. Neurons in the NTS send direct projections to hypophysiotropic corticotropin-releasing hormone (CRH) neurons and control activation of HPA axis to acute physiological, systemic stressors.

Norepinephrine (NE) action through alpha1 receptors is primarily excitatory, working directly on parvocellular neurons by increasing CRH mRNA expression via cAMP-PKA-pCREB signal transduction pathway [12]. NE may also act through presynaptic activation of glutamate release onto PVN neurons [13]. However, at higher levels of stimulation, NE effect may turn into inhibition (possibly via beta receptors). During chronic stress, lesions of ascending noradrenergic fibers attenuate stress-induced ACTH but not corticosterone release, indicating reduction in central HPA drive and increased adrenal sensitivity [14]. Glucagon-like peptide 1 (GLP-1) containing [15], prolactin-releasing peptide PrRP [16] and nesfatin [17] synthesizing noradrenergic neurons in the NTS play a broader role in stress regulation, these cells are recruited by both systemic and psychogenic stressors and involved in HPA axis sensitization under conditions of chronic stress. This neuron population -as being sensitive to metabolic cues- might also play a role in adjustment of stress response to actual energetic state of the animal [18] [14].

Neural inputs from the contiguous cell group comprising the vascular organ of the lamina terminalis (OVLT) convey information to the neurosecretory cells regarding blood borne signals related to the ion and volume homeostasis [19] and suggested as entry site for blood borne cytokines [20].

Intrahypothalamic inputs from the median eminence/arcuate region mediate nutrient- (glucose, FFA) and metabolic- (leptin, ghrelin, insulin)-associated cues. Orexigenic (NPY/AgRP) and anorexigenic (POMC/CART) cells in the arcuate nucleus are equipped with leptin, insulin and ghrelin receptors and it has been reported that leptin hyperpolarizes NPY neurons and depolarizes POMC neurons [21]. By contrast, ghrelin, acting through growth hormone secretagogue receptor stimulates AgRP and inhibits POMC neurons [22]. On the other hand, insulin receptors on AgRP neurons play an essential role in regulation of hepatic glucose production [23]. In particular, for glucose sensing, two, (electro) physiologically and functionally distinct neuron population have been identified in the CNS, which provide metabolic related information to the neurosecretory neurons. Glucose excited (GE) neurons are activated by increased glucose levels, whereas glucose inhibited (GI) neurons are stimulated when glucose levels declining [24]. In GE neurons, internalization of lactate by monocarboxylase

transporter and oxidative phosphorylation of glucose increases ATP production resulting in increased ATP/ADP ratio and in closure of KATP channels. This leads to plasma membrane depolarization and activation of voltage-sensitive Ca^{2+} channels and finally synaptic neurotransmitter release. In GI neurons, reduced ATP/ADP ratio induces the closure of chloride channels and reduction in the activity of the Na^{+}/K^{+} pumps, activation of voltage-gated Ca^{2+} channels and neurotransmitter release [25]. Among the metabolic related neurons within the arcuate nucleus, POMC neurons are glucose excited [26], while NPY/AgRP neurons are glucose inhibited [27]. Both cell types send projections to the parvocellular neurons of the PVN, and other "second order" neurons in the hypothalamus which are in the position to generate hormonal and neuronal responses to control neuroendocrine and autonomic outflow, including regulation of catecholamine discharge from the adrenal medulla.

The means with which cognitive and emotional influences evoked by psychological and social stressors regulate the hypothalamic stress-related output system are less clearly identified. The PVN is not known to receive any direct neocortical input. Aspects of the limbic system, however, have long been acknowledged as to exert a pronounced, mostly inhibitory effects on the stress-related hypothalamic neurocircuit. By contrast, amygdala, together with specific parts of the bed nucleus of stria terminalis (BNST) send direct inputs to the parvocellular subdivision of the PVN and are involved in processing and evaluation of the emotional significance of salient environmental cues. According to the recent consensus, psychogenic stressors are processed through the cortical and limbic structures and inputs from multiple limbic parts converge on regions sending direct projections to the PVN, such as the BNST or the periparaventricular GABA/glutamate-ergic interneuron population [13]. This connectivity suggests a mechanism through which information from stress-excitatory and stress-inhibitory signals are integrated to optimize the net output response [28].

Different stressors may elicit specific responses, activate different pathways [7] and it should be noted that different types of psychological challenges may recruit different stress-regulatory pathways to different degrees (**Fig.1.**) [8].

Furthermore, the stress-response, from a broader view, is not limited to the activation of the HPA axis. Restoration of the homeostasis or adaptation to novel external and

DOI:10.14753/SE.2018.2148

internal environment requires autonomic-, metabolic- behavioral- and immune adjustments. All stressors represent a threat to the homo- and allostasis, respectively, and are regarded as danger signals for the organism, which may recruit the immune system. Recently, it has become clear that exposure to stressors potentiate innate immune processes. Based on this notion, it has been hypothesized that stressor exposure change the activation status of cells of the myeloid lineage such as monocytes, macrophages, neutrophils, and microglia. However, it is not fully known how microglia, the resident macrophage population in the CNS sense and react to systemic stressful challenges. In this work I have been interested in how different stressors alter microglia and if neuron-microglia communication play a role in organizing adequate stress response.

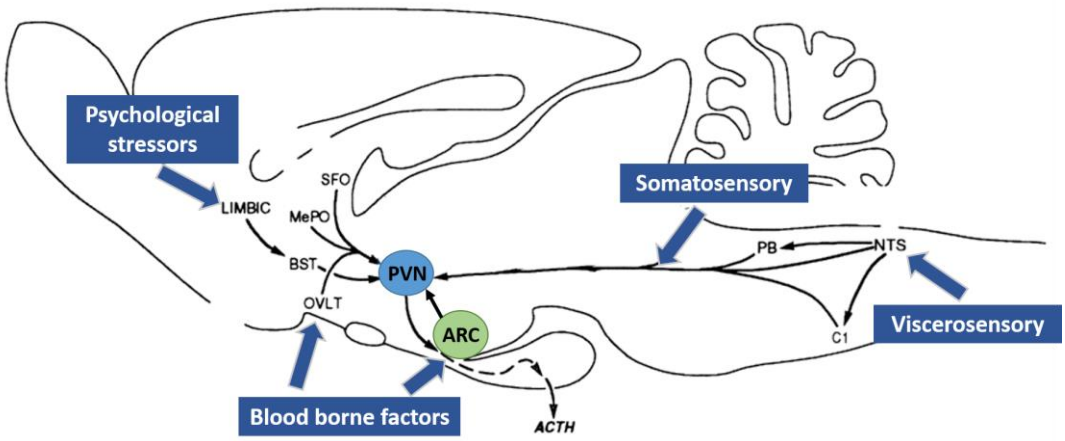

Fig.1. Afferent inputs of the hypothalamic paraventricular nucleus

Viscerosensory and somatosensorsy inputs, humoral factors and cognitive, emotional influences evoked by different stressors activate afferents pathways in the brain and at the hypothalamic level, these informations are integrated to form the appropriate response to the environmental challenges.

Abbreviations: PVN – paraventricular nucleus, ARC – arcuate nucleus, SFO - subfornical organ, MePO – median pre-optic nucleus, OVLT – vascular organ of lamina terminalis, BST – bed nucleus of the stria terminalis, PB – parabrachial nucleus, NTS - nucleus of the solitary tract, C1 – catecholaminergic group of cells in the basolateral medulla, ACTH - adrenocorticotrop hormone

2.4. Origin of microglia in the brain

Microglia represent the resident immune elements of the central nervous system (CNS). Del Rio-Hortega published a "newly identified phagocytic, migratory cells within the CNS" by using modified silver carbonate impregnation labeling [29]. He introduced the term "microglia" for the labeled cell class, and called the individual cell "microgliocyte". Glial cells were termed from the Greek word "glia" meaning glue, to suggest the "supportive" role provided by non-neuronal cells to neuronal cells. Glial cells comprise two main populations: the macroglia, which consist of astrocytes and oligodendrocytes, and the microglia.

Microglia originate from erithromyeloid progenitors (EMPs) during primitive hematopoiesis in the yolk sac at embryonic day 7.5. EMPs migrate to the neuroepithelium through blood vessels into the brain around embryonic day 8 [30] [31] where their further development is regulated by different transcription factors. In the forming CNS, factors such as IL-34 and TGF-β and engagement of CSF-1R promote microglia terminal differentiation into resident macrophages [32]. In physiological conditions, embryonic microglia maintain themselves via proliferation. However, during certain inflammatory conditions that alter blood-brain barrier (BBB) integrity, the recruitment of monocytes or other bone marrow-derived progenitors can supplement the microglial population [33].

2.5. Neuron-microglia communication in the brain

Traditionally, microglia were thought to be "resting" or "quiescent" and becoming "activated" upon perturbations in CNS homeostasis, by which they undergo rapid morphologic and functional transformation. However, modern microscopic techniques, in vivo imaging revealed that microglia are highly motile in their default state [34, 35] . Wake et al. showed that microglia processes make brief contacts (circa 5 min) with neuronal processes about once per hour, suggesting the role of microglia in monitoring the functional state of neurons [36]. Therefore, Hannish and Kettenmann suggested that the baseline state of microglia is "surveying" rather than "resting" [37].

Microglia-neuron communication goes on between these cells in both directions. Microglia make physical contacts not only with dying neurons but also with neuronal elements under physiological conditions and release certain paracrine signals. It is

important to keep in mind, that information processing in the synapses is not only defined by neurones, but also by astrocytes, which enfold the synapses and by microglia, which dynamically interact with synapses. The motile microglial processes, with the more immobile processes of astrocytes, and the pre- and postsynaptic neuronal elements form a "quad-partite" synapse (**Fig.2**.). In turn, neurons can modulate microglial activation state by purinergic signaling, classic neurotransmitters, micro-RNA (mir-124) and chemokines (CD200, CX3CL1) [38]. Under physiological conditions microglia are suppressed by "off" signals (CD200, CX3CL1, CD22) that are produced by neurons to keep microglia in the default, surveying state [38]. In contrast, "on" signals originating either from neurons or other cell types (purines, glutamate, chemokines) or from exogenous factors (pathogen-associated molecular patterns – PAMP, danger-associated molecular patterns - DAMPS) induce microglia activation [39-41].

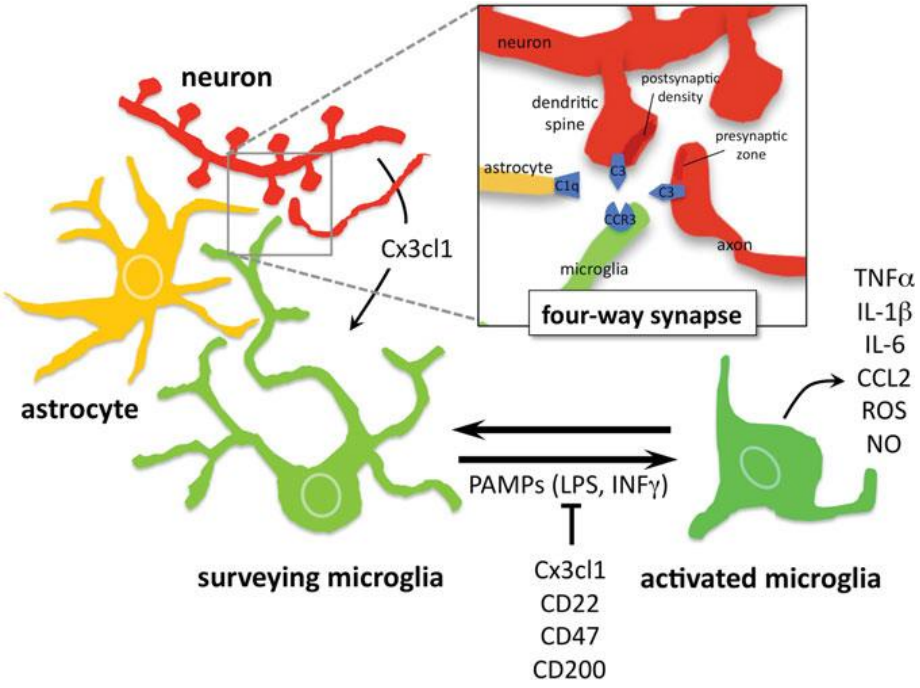

Fig.2. The four-way synapse and the inhibitory/ stimulatory signals of microglial activation

The four-way synapse containing neuronal elements and processes of astrocytes and microglial cells. The "off" signals that keep microglia in surveying state and "on" signals that induce microglia activation [38]

Activation of microglia imply robust changes in cell shape (retraction of long processes, changing number of branches, in extreme case transformation into an amoeboid shape), rapid migration to the site of damage [38]. Microglia can express a broad pattern of cytokines and change their MHC expression profile [39, 40]. Activated microglia are able to express different spectra of pro- or anti-inflammatory cytokines depending on circumstances. Microglia can exhibit anti-inflammatory phenotype, secreting neurotrophic factors, promoting neuroprotection, neurogenesis and glia development. However, microglia is a "two-edged sword" [42], because certain pathological conditions (pathogen insult, ischemic stroke or neurodegenerative disease) can drive microglia into an activated proinflammatory phenotype. Microglia, releasing proinflammatory factors (IL-1β, IL-6, TNF-α, ROS, NO) induce exaggerated inflammation [43, 44], moreover, in some cases the fully activated microglia have neurotoxic effect (Parkinson-disease) [45].

2.6. Fractalkine/ Fractalkine receptor

Among the pathways mediating environmental cues through neuron-microglia crosstalk [46] the fractalkine (CX_3CL1)-fractalkine receptor (CX_3CR1) signaling plays a crucial role [47, 48].

Fractalkine is the only member of CX_3C chemokine family, which is synthesized as a transmembrane protein with the CX_3C chemokine domain and an extended highly glycosylated, mucin-like stalk [49]. It is found either in membrane bound or secreted forms. The two forms have distinct functions, the membrane bound form is involved in cell-cell adhesion, while the secreted form plays a role in chemotaxis of circulating cells expressing its receptor (CX3CR1) [50]. Fractalkine might have neuroprotective or neurotoxic profile in the CNS [51]. Proteolytic cleavage of fractalkine is promoted by the disintegrin-like metalloproteinase ADAM10 [52] or, under inflammatory conditions, by ADAM17/TACE [53] resulting in shed CX_3CL1 entities. CX_3CL1 is expressed at the periphery in the intestinal epithelium, endothelium, lung, kidney, pancreas, liver, adipose tissue in physiological conditions, and it is upregulated in inflammatory conditions [54-60]. Fractalkine is expressed in the CNS constitutively and abundantly in cell-type specific manner on neurons [47] but it can be induced by TNFα and IFNγ treatment in astrocytes as well [61].

DOI:10.14753/SE.2018.2148

Fractalkine interacts with its unique Gαi-coupled seven-transmembrane receptor [47, 62]. Fractalkine receptor is expressed on cells of the myeloid linage, including monocytes and macrophages and its expression has also been described on NK cells and on certain T cell populations at the periphery [62]. CX_3CR1 is restricted to microglial cells in the CNS [63].

2.7. Fractalkine receptor deficient mice

Functional studies on fractalkine signaling have been significantly promoted by the development of transgenic mouse line in which the *cx3cr1* gene has been replaced by the marker gene encoding *egfp* [64]. Heterozygous mice $CX_3CR1^{+/gfp}$ do not display behavioral or immune phenotype, however can be used as a reporter of microglia activity. By contrast, homozygous mice, $CX_3CR1^{gfp/gfp}$ have no functional receptor. $CX_3CR1^{-/-}$ mice show increased repetitive behavior and impaired social recognition due to decreased connectivity between prefrontal cortex and other brain areas. These behavioral differences are thought to be due to transient decrease of microglia recruitment in a critical neurodevelopmental period and associated with defects in synaptic pruning [65]. Although CX_3CR1 deficient mice display increased LTP at CA1 and perform better in Morris water maze than wild type animals, they are resistant to the effects of enriched environment [66]. $CX_3CR1^{-/-}$ mice display lasting sickness behavior and exaggerated brain cytokine response in response to single LPS injection [67].

Recently, several new features of microglia function emerge. At the beginning of my work only a few report described activated microglia in the limbic system of stressed rodents, without any indication on their modulatory role in the complex hypothalamic stress regulation. With the $CX_3CR1^{-/-}$ mice tools became available with which to address the following questions:

DOI:10.14753/SE.2018.2148

3. Objectives

I aimed to clarify if acute/chronic exposure of psychogenic or physiological stressful stimuli activate microglia in the hypothalamus, the major integrator of stress response.

My second aim was to investigate if neuron-microglia communication plays a role in organizing adequate stress response.

Therefore, my **specific aims** were to determine if the fractalkine/ fractalkine receptor signaling pathway:

- influences the coping strategy or anxiety- and depressive-related behavior evoked by acute or chronic psychological stress?
- contributes to hormonal stress responses and microglial activation in the hypothalamus induced by acute/chronic psychogenic or physiological challenges?
- has an effect on metabolic phenotype, and counter-regulatory responses induced by insulin-induced hypoglycemia?

DOI:10.14753/SE.2018.2148

4. Methods

4.1. Animals

Experiments were performed in adult (64-100 days old) male C57BL/6 and fractalkine receptor deficient, $CX_3CR1^{-/-}$ ($CX_3CR1^{gfp/gfp}$) mice. Fractalkine receptor deficient mice were obtained from the European Mouse Mutant Archive (EMMA EM00055), on C57BL/6 background [64]. In these mice, the *cx3cr1* gene was replaced by a *gfp* reporter gene. Adult (60-100 days old) male IL-1a/b knockout (KO) mice [68], on C57BL/6 background were also used to test the effect of interleukin-1 (IL-1) on glycemic control. Animals were bred at the Specific Pathogen Free (SPF) level as heterozygote breeder pairs, and were maintained at the Minimal Disease level of the Transgenic Facility of our Institute. The genotype of the animals was determined by TaqMan rtPCR using Thermofisher EGFP assay (ID: Mr00660654_cn) in a multiplex reaction with Mouse TaqMan® Copy Number Reference Assay as an internal standard. Animals had free access to standard laboratory animal chow and water and were kept under temperature-, humidity-, and light controlled conditions (21°C± 1°C, 65% humidity, 12-h light/12-h dark cycle, with lights on at 07:00 hours). All procedures were conducted in accordance with the guidelines set by the European Communities Council Directive (86/609 EEC) and approved by the Institutional Animal Care and Use Committee of the Institute of Experimental Medicine.

4.2. Analysis of metabolic parameters

Mice (n=8 per genotype) were singly housed in TSE Phenomaster cages (TSE Systems GmbH Bad Homburg, Germany) and acclimatized for 1 day followed by 72 hours data collection of food consumption, X-Y-Z locomotor activity, oxygen consumption (ml/h/kg) (VO_2) and CO_2 production (ml/h/kg) (VCO_2). Energy expenditure (EE (kcal/h)) was calculated using a rearrangement of the abbreviated Weir equation as supplied by TSE Labmaster System: EE= [3.941 (VO_2) + 1.106 (VCO_2)] x 1.44. The respiratory exchange ratio (RER) was calculated as VCO_2/VO_2.

DOI:10.14753/SE.2018.2148

4.3. Behavior tests

C57BL/6 and $CX_3CR1^{-/-}$ mice (n=36 per genotype) were compared in four behavior tests: open field test, elevated plus maze test, forced swim test and tail suspension test.

All behavioral testing was performed in the early light phase of the day in a separate quiet testing room under approximately 400 lx light intensity, which was similar to that employed in the maintenance rooms. Behavioral tests were video recorded with a Panasonic SDR-H90 digital camcorder and analyzed later with the H77 computer based event recorder software (Jozsef Haller, Institute of Experimental Medicine, Budapest, Hungary).

4.3.1. Open-field test (OF)

The open field was a white, non-transparent plastic box (40 x 40 x 30 (height) cm.). Mice (C57BL/6, n=8; $CX_3CR1^{-/-}$, n=8) were placed in the center of the box and allowed to explore the apparatus for 10 min. Locomotion was assessed by counting the crossing of the lines of a 4 x 4 grid that divided the open field into 16 squares (each square was 10 x 10 cm). Lines were drawn on the video screen, and were not visible to the mice. Exploration in the central area was also recorded to provide an additional measure for anxiety-like behavior in the open field. Four inner squares of the grid were considered as central area. The apparatus was cleaned with tap water and paper towel between subjects.

4.3.2. Elevated plus-maze test (EPM)

The elevated plus-maze (arm length=30 cm, arm width=7 cm; wall height=30 cm; platform height=80 cm) was made of dark-grey painted plexiglas. Open arms were surrounded by 0.3 mm high ledges. Mice (C57BL/6, n=7; $CX_3CR1^{-/-}$, n=7) were placed into the central area of apparatus with its head facing one of the open arms and were allowed to explore the apparatus for 5 min. Percentage of time spent in open arms was used as measure of anxiety, whereas the ratio of the open arm entries to the total entries were considered indicators of locomotor activity. Mice were considered to enter a compartment when all four legs crossed the lines separating the compartments. The apparatus was cleaned with tap water and paper towel between tests.

4.3.3. Forced swim test (FST)

Mice (C57BL/6, n=14; $CX_3CR1^{-/-}$, n=16) were forced to swim for 6 min in 18 cm high and 14 cm diameter glass cylinders filled with clean tap water heated to 24.5±1 °C. After swimming, mice were dried with paper towels, and a clean paper towel was left in the home cage for at least an hour to avoid cooling. Water was changed and cylinders were cleaned between subjects. In this test, the time spent either being immobile floating at the surface or swimming and struggling has been measured. *Floating* was defined as being stationary with only enough motion of the tail or forepaws to keep the head above water. *Swimming* was defined as active use of the forepaws with forward movement, in the center or along the sides of the cylinder, which did not involve lifting the paws above the surface of the water. During swimming, the body is usually oriented parallel to the sides of the cylinder. *Struggling* was defined as active pawing of the side of the cylinder, lifting the paws above the surface of the water. Here, animals are facing towards the wall and the body oriented perpendicularly to the side of the cylinder. The animals were not pre-exposed to forced swim before testing.

To measure forced swim stress-induced plasma hormone levels, a second set of mice (C57BL/6, n=6; $CX_3CR1^{-/-}$, n=6) were forced to swim for 6 min and decapitated, trunk blood was collected into chilled plastic tubes containing 10 µl of 20% K-EDTA and centrifuged.

4.3.4. Tail suspension test (TST)

TST was performed using a computerized device system (ID-TECH-BIOSEB) consisting of three compartments with two suspension units in each compartment. Mice (C57BL/6, n=7; $CX_3CR1^{-/-}$, n=5) were suspended by the tail (with adhesive Scotch tape) in the TST apparatus. The tail suspension test is based on the fact that animals subjected to short term, inescapable challenge of being suspended by their tail, will develop an immobile posture. The test lasted for 6 min. The apparatus recorded three parameters: duration of immobility, mechanical energy- and power of the movements. The *duration of immobility* is the main parameter measured. This is calculated from the cumulated time during which the animals movements do not exceed the threshold determined by the level filtering device. The *power of the movements* is calculated from the total

mechanical energy of the movements by the animal during the test, divided by the total time the animal is active (arbitrary units).

4.4. Acute restraint stress

Restraint stress was performed using transparent ventilated Falcon tubes fitted to the size of the animals. Packing with paper towels at the rear was used to achieve comparable degree of restraint. This procedure minimized the space around the animal, prevented them from turning and provided stressful stimulus, without being harmful. Due to distinct time course of hormonal and activational markers [12], restrained mice were sacrificed at 15 min for ACTH and corticosterone measurement (C57BL/6, n=6; $CX_3CR1^{-/-}$, n=6) and after 90 min for c-Fos and Iba1 immunocytochemistry (C57BL/6, n=5; $CX_3CR1^{-/-}$, n=5).

4.5. Two-hit stress protocol

Two-hit stress protocol is a combination of early life adversity (maternal separation, MS) followed by chronic variable stress (CVS) paradigm in the adulthood. This protocol has been repeatedly shown to induce anxiety/depression-like symptoms in laboratory rodents [69]. MS protocol was adopted from Veenema et al. [70]. Briefly, pups were separated daily between 09:00 and 12:00 h from their dams for 3 h from postnatal d 1–14. First, dams were removed from the maternity cage and placed into separate individual cages. Pups were then removed as complete litters from the nest, transferred to an adjacent room, and put into a small box placed on a heating pad (30–33 ^{o}C). After the 3-h separation period, pups were returned to the home cage followed by reunion with the dam. Unseparated control (Control) litters were left undisturbed, except for change of bedding once a week. Pups were taken from twelve (C57BL/6) or eight ($CX_3CR1^{-/-}$) control litters and ten (C57BL/6) or nine ($CX_3CR1^{-/-}$) MS litters. Pups were weaned at postnatal day 21 and housed in groups of four to five until the start of chronic variable stress procedure (CVS).

CVS is a commonly used paradigm designed to introduce recurrent physical, psychological and social stress that is unpredictable and unavoidable [71]. In the CVS paradigm used here, mice were exposed to two stressors daily for 3 weeks according to the schedule in **Table 1**. Each stressor was randomly presented no more than 5 times. Exposing mice to different stressful stimuli prevented habituation to stress. At the end

of the stress procedure, all mice were tested in sucrose consumption and in the open field tests. EthoVision XT video tracking software (version 10.1.856) (Noldus Information Technology, Wageningen, The Netherlands) was used to analyze the open field behavior. In each video, the mouse was detected and the software then autonomously tracked animal movement from the perspective of the center point of the animal's body to quantify the total distance traveled by each mouse.

Body weight was measured before CVS exposure and 3 weeks later, before decapitation. The body weight change was calculated as a difference between these two values.

DOI:10.14753/SE.2018.2148

Table 1. The stressors of chronic variable stress procedure and the behavior tests

Chronic Variable Stress (CVS) Schedule

Day	Morning	Afternoon
D0	***Sucrose consumption test***	
D1	Restraint (1h)	Footshock (0,5 mA; 1s every 20s; 12 min)
D2	Social defeat (2h)	Lights on (overnight)
D3	Forced swim test (5 min, 25 C°)	Tilted cage (overnight)
D4	Shaker (60 rpm)-Overcrowding (1h)	Overcrowding-Lights off (overnight)
D5	Restraint-Shaker (60 rpm) (1h)	Social isolation (overnight)
D6	Social defeat (1h)	Forced swim test (5 min, 25 C°)
D7	Shaker (60 rpm)-Overcrowding (1h)	Footshock (0,5 mA; 1s every 20s; 12 min)
D8	Social defeat (1h)	Tilted cage-Wet bedding (overnight)
D9	Restraint (1h)	Lights on (overnight)
D10	Shaker (60 rpm)-Overcrowding (1h)	Overcrowding-Tilted cage-Rat odor(overnight)
D11	Social isolation	Social isolation-Lights off (overnight)
D12	Forced swim test (5 min, 25 C°)	Footshock (0,5 mA; 1s every 20s; 12 min)
D13	Overcrowding-Wet bedding (2h)	Tilted cage- Rat odor (overnight)
D14	Restraint (1h)	Social defeat (1h)
D15	Shaker (60 rpm)-Overcrowding (1h)	Lights off (overnight)
D16	Footshock (0,5 mA; 1s every 20s; 12 min)	Lights on (overnight)
D17	Restraint (1h)	Overcrowding-Wet bedding (overnight)
D18	Social defeat (1h)	Lights off (overnight)
D19	Footshock (0,5 mA; 1s every 20s; 12 min)	Social isolation (overnight)
D20	***Open field test (10 min)***	
D21	***Elevated plus maze test (5min)***	
D22	***Sucrose consumption test***	

4.6. Sucrose consumption test

Sucrose preference test was performed just before CVS exposure and at the end of chronic stress procedure, 20 days later. During this test, mice were given, for 24 h, a free choice between two bottles, one with 1% sucrose solution and another with tap water. To prevent possible effects of side preference in drinking behavior, the position of the bottles was switched after 12 h. No previous food or water deprivation was applied before the test. The consumption of fluids was measured by weighing the

bottles, and the sucrose preference was calculated as a percentage of consumed sucrose solution of the total amount of liquid drunk.

4.7. Hypoglycemic stress

Following overnight fast, insulin (1.0 IU/kg, Actrapid) or saline was injected intraperitoneally. At 60 minutes after insulin administration mice were either transcardially perfused for in situ hybridization and c-Fos plus Iba1 double immunocytochemistry or were decapitated for collecting samples for ACTH, CORT measurements and RT-qPCR. Samples were stored at -70 °C until measurements.

4.8. Intracerebroventricular injection

Three experiments were conducted. In the first experiment, mice were divided into two groups (n = 5/5 per group): icv. saline + ip. [saline+insulin] or icv. minocycline + ip. [minocycline+insulin]. Following overnight fasting, ip. insulin (0.8 IU/kg, Actrapid) was administered on the next day as icv. injection. In the second experiment, after 150 min of food deprivation, mice (n = 3/2 per group) received IL-1RA (n = 8/8 per group) or icv. saline once prior to and two hours later ip. insulin injection (0.8 IU/kg, Actrapid).

C57BL/6 mice were deeply anesthetized with an ip. injection of sodium ketamine hydrochloride (100 mg/ml)/xylazine (20 mg/ml) solution. The top of the skull was shaved to remove fur and mice were then placed in a stereotaxic device. Surgical site was swabbed with betadine solution and then with 70 % alcohol. A single dose of icv. minocycline (Sigma-Aldrich, 20 µg/total volume of 2 µl), or IL-1RA (Anakinra; Kineret, 100mg/0,67ml; SOBI) was injected into the right lateral ventricle of the brain using the stereotaxic apparatus. The sham groups received an icv. injection of saline solution (total volume of 2µl). The bregma coordinates used for the injection were -1.0 mm lateral, -0.5 mm posterior, -2.5 mm below.

4.9. High-fat diet

22-25 days old mice were fed with normal diet (ND) or high-fat diet (HFD) for 10 weeks. The first group, normal diet (ND), received standard chow (VRF1 (P), Special Diets Services (SDS), Witham, Essex, UK.). The second group received high-fat diet (HFD), by providing a 2:1 mixture of standard chow and lard (Spar Budget, Budapest, Hungary). The energy content and macronutrient composition of the two diets is given

in Table 2. Body weight was regularly measured, and mice were transcardially perfused (n= 4-4). A separate set of obese and lean mice underwent cold tolerance test.

Table 2. Energy content and macronutrient composition of diets

	ND - standard chow		**HFD - mixed chow**	
	g%	kcal%	g%	kcal%
Protein	19,1	22,5	12,7	9,7
Carbohydrate	55,3	65,0	36,9	28,0
Fat	4,8	12,6	36,5	62,3
kcal/g	3,40		5,27	

4.10. Cold stress and core body temperature measurement

Rectal temperature was measured with Multithermo thermometer (Seiwa Me Laboratories Inc., Tokyo, Japan). To assess cold tolerance, set of animals (n = 30) from both genotypes were fasted for 5 hours, then placed into new individual cages with minimal bedding and transferred to cold room (4^{o}C). Rectal temperature was measured before and 60, 120, 180 and 240 min after cold exposure.

4.11. Tissue processing

Under terminal anesthesia (Nembutal, Ceva-Phylaxia, Budapest, Hungary), animals were transcardially perfused with saline (0.9% NaCl) followed by 40 mL ice-cold fixative (4% paraformaldehyde in 0.1M borate buffer, pH 9). Brains were removed, post-fixed (in the same fixative for 3 h) and cryoprotected overnight in 10% sucrose (in 0.1M phosphate-buffered saline, PBS) at 4 ˚C. Four series of coronal sections (25 μm) were cut on freezing microtome. Sections were stored at −20 ˚C in antifreeze solution (containing 30% ethylene glycol and 20% glycerol in 0.1M PBS).

4.12. c-Fos and Iba1 immunocytochemistry

c-Fos (n=5-6/group) or Iba1 immunoreactivity (n=5-6/group) was revealed by conventional avidin–biotin–immunoperoxydase protocol. Free-floating brain sections were incubated sequentially in (a) 1% hydrogen peroxide (H_2O_2) in distilled water for 10 min; (b) 2% normal goat serum (Vector Laboratories, Burlingame, CA) in PBS/0.3% Triton X100 at room temperature for 1 h; (c) rabbit anti-c-Fos IgG (sc-52 Santa Cruz Biotechnology, Santa Cruz, CA, 1:20000) at 4 °C for 72 h or rabbit anti-Iba1 (019-19741, Wako Chemicals GmbH, Neuss, Germany, 1:1000 dilution) primary antibody at 4 °C overnight;(d) biotinylated goat anti-rabbit IgG (Vector Labs, 1:200 dilution) at room temperature for 60 min; (e) avidin–biotin–horse radish peroxidase complex (Vector Labs, 1:200 dilution) at room temperature for 60 min. The resulting peroxidase activity was developed in 3,3 -diaminobenzidine (DAB, Sigma). Sections were mounted onto slides, dehydrated in alcohols, cleared with xylene and coverslipped.

4.13. Double immunofluorescence for c-FOS and SMI 32 immunoreactivity

To examine the connection of GFP+ microglial cells with with c-Fos positive neurons, double-labeling immunofluorescence was performed on free-floating brain sections from heterozygote $CX_3CR1^{+/-}$ mice which express GFP and maintain receptor function in CX3CR1 expressing cells. After pre-incubating in 2% normal donkey and horse serum (60 min, at room temperature), sections were incubated in a mixture of rabbit anti-c-Fos IgG (sc-52 Santa Cruz Biotechnology, Santa Cruz, CA, 1:2000) and mouse anti-neurofilament [SMI 32] IgG (BioLegend, 1:500) at 4 °C overnight. The antigens were then visualized by biotinylated horse anti-mouse IgG (Vector Labs, 1:500) for 1 hour followed by streptavidin Alexa 405 (Molecular Probes, 1:500) and donkey anti-rabbit IgG conjugated with Alexa Fluor 594 (Invitrogen, 1:500) for 3 hours. After washing, the sections were transferred to slides, and covered with Fluoromount-G™ Solution (Southern Biotechnology Associates).

Fluorescent images were taken by confocal laser scanning using a Nikon C2+ microscope, brightfield images were captured at 20x magnification by Spot RT color digital camera (Diagnostic Instruments Inc., IL, USA) on Nikon Eclipse 6000 microscope. The apposition of GFP positive microglial processes to c-Fos positive

neurons were evaluated at the arcuate nucleus by using Z-stack imaging. Three-dimensional image analysis was carried out by using NIS-Elements Viewer 4.2 software.

4.14. Imaging, quantification and data analysis

One complete series of regularly spaced sections (4x25µm=100 µm apart) were stained for each antigens. Digital images of both sides of the PVN as defined by the Paxinos and Franklin's mouse brain atlas (between bregma -0.58 and -0.94) and ARC (between bregma -1.22 and -1.94) in C57BL/6 and $CX_3CR1^{-/-}$ mice were captured 20x magnification by Spot RT color digital camera (Diagnostic Instruments Inc., IL, USA) on Nikon Eclipse 6000 microscope. Images were then re-opened in Image J software and set at a common threshold to subtract the background optical density and the numbers or the area of the immunopositive profiles above the background were counted. The region of interest (PVN) was outlined by a 0,390 mm x 0,290 mm rectangle selection tool with the top of the rectangle positioned in line with the tip of the 3rd ventricle. ARC was outlined by 0,290 mm x 0,290 mm rectangle selection tool with the top of the rectangle positioned in line with the bottom of the 3rd ventricle. The software allowed us to determine the number of immunoreactive cell nuclei (c-Fos) or Iba-1 positive microglia within the region of interest. 3-4 sections per animal were used in the analysis. Quantitation was performed in a blinded fashion.

The number of c-Fos positive cells was automatically counted using the ImageJ 1.48 software after outlining the unit region of interest and thresholding all sections to a common level. ImageJ "Watershed" function, an automatic separation tool was used to separate fused cells by a 1 pixel line. The minimum size of a profile to be considered as a c-Fos-positive cell nucleus was determined as more than 45 pixels. Total cell counts were taken bilaterally at regularly spaced intervals and expressed as mean±SEM for each treatment group.

The area of Iba1+ profiles and the density of Iba1+ microglia (number of cells/mm^2) was analyzed using ImageJ 1.48 software. Quantification of Iba1+ cells were performed in the region of interest using unit area rectangle selection over the PVN area. All imaging parameters were the same for each image. The images were converted into a binary black-and-white format using the ImageJ processing tool. "Make binary" with an

automated threshold (‘‘default” threshold, a variation of the IsoData algorithm also known as iterative intermeans). An automated count of black pixels (representing all Iba1+ signals) was applied and the Iba1 staining was reported as percentage of unit area. Distribution of microglia in the hypothalamus was characterized by the spacing index, calculated from the distance between the neighboring microglia [72]. For this calculation, the X-Y coordinates for each microglia were recorded at the unit region of interest using the automark function of the ImageJ program and fed into Matlab R2016a program. The Euclidean distance between each microglia and its nearest neighbor (NND) was calculated in Matlab Program, after that averaged, squared and multiplied by the density of Iba1+ microglia. This value was then averaged for all images to define the value per animal.

4.15. c-Fos and Iba1 double immunohistochemistry

c-Fos and Iba1 immunoreactivity was revealed by conventional avidin–biotin–immunoperoxydase protocol. Free-floating brain sections were incubated sequentially in (a) 1% hydrogen peroxide (H_2O_2) in distilled water for 10 min; (b) 2% normal goat serum (Vector Laboratories, Burlingame, CA) in PBS/0.3% Triton X100 at room temperature for 1 h; (c) rabbit anti-c-Fos polyclonal IgG (sc-52 Santa Cruz Biotechnology, Santa Cruz, CA, 1:10000) at 4 ◦C for 40 h; (d) biotinylated goat anti-rabbit IgG (Vector Labs, 1:200 dilution) at room temperature for 60 min; (e) avidin–biotin–horse radish peroxidase complex (Vector Labs, 1:200 dilution) at room temperature for 60 min. c-Fos immunoreaction was visualized by using nickel-intensified 3,3 -diaminobenzidine reaction (DAB, Sigma).

After extensive washing steps, sections were incubated in anti-Iba1 antibody (rabbit polyclonal, WAKO, 1:1000). Iba1 immunoreaction was developed in diaminobenzidine (DAB, Sigma) only. This combination resulted in black cell nuclear staining corresponding to activated cells and microglia appeared as brownish cytoplasmic staining. Sections were mounted onto slides, dehydrated in alcohols, cleared with xylene and coverslipped.

4.16. Combined Immunohistochemical Labeling and In Situ Hybridization (ISH)

Two series of hypothalamic sections of each mice were processed for c-Fos immunohistochemistry and ISH for NPY or POMC mRNA. The procedure is a variant of a protocol described by Simmons et al. [73]. In brief, immunolocalization of c-Fos protein was carried out as described above, except that the tissue was not pretreated with H_2O_2. In addition, the incubation step in normal serum was omitted, the sections were placed into the primary antiserum supplemented with 3% bovine serum albumin as a blocking agent and with 5 mg/ml heparine to inhibit RNase activity. The DAB reaction was developed without nickel intensification. Immunostained sections were then mounted on slides and in situ hybridization was carried out as described above. pBLNPY-1 plasmid contains a 511 bp insert comprising most of the cDNA of mouse prepro-neuropeptide Y ligated into the Eco RI site of the Bluescribe M13 (-) vector. Antisense RNA transcript was prepared by the use of T3 RNA polymerase. Radiolabeled (^{35}S-UTP) cRNA probe was used for detection the expression of NPY mRNA. c-Fos immunolabeled tissue sections were mounted onto SuperFrost Ultra Plus (Menzer–Glazer) slides thereafter post-fixed with 4% paraformaldehyde in 0.1M borate buffer, pH= 9, digested with Proteinase K (Sigma, 10mg/mL in 50mmol/LTris, pH= 8 and 5mmol/L EDTA at 37 ◦C, 5 min), acetylated (0.25% acetic anhydride in 0.1 mol/L triethanolamine, pH= 8), and dehydrated. Hybridization mixture (50% formamide, 0.3 mol/L NaCl, 10 mmol/L Tris (pH = 8), 2mmol/L EDTA, 1× Denhardt's, 10% dextran sulfate, 0.5mg/mL yeast tRNA) was pipetted onto the slides (100 mL, containing probe at 107 d.p.m./mL) and hybridized overnight at 56 ◦C. Sections were then rinsed in 4× SSC (1× SSC: 0.15 mol/L NaCl and 15 mmol/L trisodium citrate buffer SSC, pH= 7), digested with ribonuclease A (Sigma, 20mg/mL in Tris–EDTA buffer with 0.5 mol/L NaCl at 37 ◦C for 30 min), gradually desalted, and washed in 0.1× SSC at 65◦ for 30 min, dehydrated and air dried. Hybridized sections were dipped into Kodak NTB-3 emulsion and exposed for 5 days.

4.17. Gene expression analysis by quantitative real-time PCR

Mice (n=3-4) were decapitated, the whole hypothalamic blocks or arcuate nucleus regions were dissected and frozen immediately at -70^{o}C. Total RNA was isolated with QIAGEN RNeasyMiniKit (Qiagen, Valencia, CA, USA) according the manufacturer's instruction. To eliminate genomic DNA contamination, DNase I (Fermentas) treatment was used. Sample quality control and the quantitative analysis were carried out by NanoDrop (Thermo Scientific). cDNA synthesis was performed with the High Capacity cDNA Reverse Transcription Kit (Applied Biosystems, Foster City, CA, USA). The designed primers (Invitrogen) were used in real-time PCR reaction with Power SYBR Green PCR master mix (Applied Biosystems, Foster City, CA, USA) on ABI StepOnePlus instrument. The gene expression was analyzed by ABI StepOne 2.3 program. The amplicon was tested by Melt Curve Analysis. Measurements were normalized to GAPDH expression. Amplification was not detected in the RT-minus controls. Primers used for the comparative CT (threshold cycle) experiments were designed by the Primer Express 3.0 program. Primer sequences for the following genes are:

GAPDH:

(f) TGACGTGCCGCCTGGAGAAA

(r) AGTGTAGCCCAAGATGCCCTTCAG

CRH mRNA:

(f) CGCAGCCCTTGAATTTCTTG

(r) CCCAGGCGGAGGAAGTATTCTT

NPY mRNA:

(f) CAGATACTACTCCGCTCTGCGACACTACAT

(r) TTCCTTCATTAAGAGGTCTGAAATCAGTGTCT

POMC mRNA

(f) CGAGATTCTGCTACAGTCGCTCAGG

(r) GCCAGGAAACACGGGCGTCT

AGRP mRNA

(f) AGGACTCGTGCAGCCTTACAC

(r) AGCTTTGGCGGCGGTGCTA

Iba1 mRNA

(f) AGCTGCCTGTCTTAACCTGCATC

(r) TTCTGGGACCGTTCTCACACTTC

IL-1a mRNA

(f) CCATAACCCATGATCTGGAAGAG

(r) GCTTCAGTTTGTATCTCAAATCAC

IL-1b mRNA

(f) CTC GTG GTG TCG GAC CCA TAT GA

(r) TGA GGC CCA AGG CCA CAG GT

4.18. ACTH and corticosterone measurement

After decapitation, trunk blood was collected into chilled plastic tubes containing 10 µl of 20% K-EDTA, centrifuged and plasma samples were stored at −20 ˚C until hormone measurements. ACTH and corticosterone were determined using a direct radioimmunassay (RIA) as described [74, 75].

4.19. Catecholamine determination

Catecholamines (epinephrine, norepinephrine) were analyzed in individual plasma samples or pooled plasma samples. To obtain a pooled plasma sample, equal volumes of each individual sample (n=3/4 per group) from the same experimental group were mixed. Samples were used for the catecholamine measurements using 2-CAT ELISA kits (Labor Diagnostica Nord, Nordhorn, Germany).

4.20. Cell culture

Mouse microglial BV2 cell line was obtained from the Cell Culture Core Facility at the Institute of Experimental Medicine and cultured in humidified atmosphere of 5%CO2 in DMEM/F12 (1:1) media with 10% FCS containing Glutamax and penicillin/streptomycin. Cells were trypsinized and plated in multi-well plates before appropriate treatments. Cells were treated with 2-DG (Sigma) 1 and 10 mM for 3h or

insulin 1nM overnight and harvested. IL-1 mRNA expression was measured by qPCR as described above.

4.21. Statistical analysis

Statistical analysis was performed using GraphPad Prism software (ver. 6.01; San Diego, CA, USA) using two-way ANOVA with Bonferroni post hoc test. To determine the significant differences between the two group means, unpaired, two sided t-test was performed. If the populations had significantly different standard deviation, data were analyzed by unpaired t test with Welch's correction. P-value < 0.05 was considered statistically significant. On the figures, * marks genotype difference, # marks treatment effects. Data are expressed as group means ± standard error of the mean (SEM).

DOI:10.14753/SE.2018.2148

5. Results

5.1. Effects of acute psychological stress on fractalkine receptor deficient mice ($CX_3CR1^{-/-}$)

5.1.1. Home cage locomotor activity and behavior tests with acute stress component

5.1.1.1. Home cage activity

There was a significant circadian difference between day/night locomotor activity and speed of the movements in the home cage, but we did not detect any significant difference between wild-type (C57BL/6) and fractalkine receptor deficient mice ($CX_3CR1^{-/-}$) neither in the light, nor in the dark phase of the day ($p<0.05$) (Fig. 3A). There was also no significant genotype effect on the average speed of the movements (Fig. 3B).

5.1.1.2. Open field test

As shown on Fig. 3C there was no difference in the locomotor activity between genotypes in the open field [$t(26)=0.6502$, $p>0.05$], and we did not detect any significant difference between C57BL/6 and $CX_3CR1^{-/-}$ mice in the time spent in the center [$t(26)=0.8942$, $p>0.05$] (Fig. 1D).

5.1.1.3. Elevated plus maze test

As shown in Fig. 3F, preference for open arms of homozygous fractalkine receptor deficient ($CX_3CR1^{-/-}$) mice showed a trend towards less anxious phenotype, but the open arms' time was not statistically different from wild-type mice (C57BL/6) [Welch-corrected $t(16.57)=1.546$, $p>0.05$]. $CX_3CR1^{-/-}$ mice did not spend more time in the open arms than wild-type mice [Welch-corrected $t(15.07)=1.750$, $p=0.1005$] (Fig. 3E).

5.1.1.4. Forced swim test

$CX_3CR1^{-/-}$ mice displayed active coping behavior during forced swimming. These mice exhibited significantly decreased immobility in the forced swim test when compared with wild-type animals [$t(28)=2.179$, $p=0.0379$] (Fig. 3G); spent significantly more time

struggling (Fig. 3H) [t(28)=2.269, p=0.0312], while there was no difference in the duration of swimming [t(28)=0.344, p=0.733] (Fig. 3I).

5.1.1.5. Tail suspension test

The fractalkine receptor deficient mice were more active to escape in the tail suspension test. In this test, $CX_3CR1^{-/-}$ mice spent less time in immobility than wild-type mice [t(16)=2.506, p=0.0234] (Fig. 3J). However, the difference between the genotypes in the latency of immobility was not significant [t(16)=0.6659, p>0.05] (Fig. 3K). The power of their movements was not different between the examined genotypes (Fig. 3L).

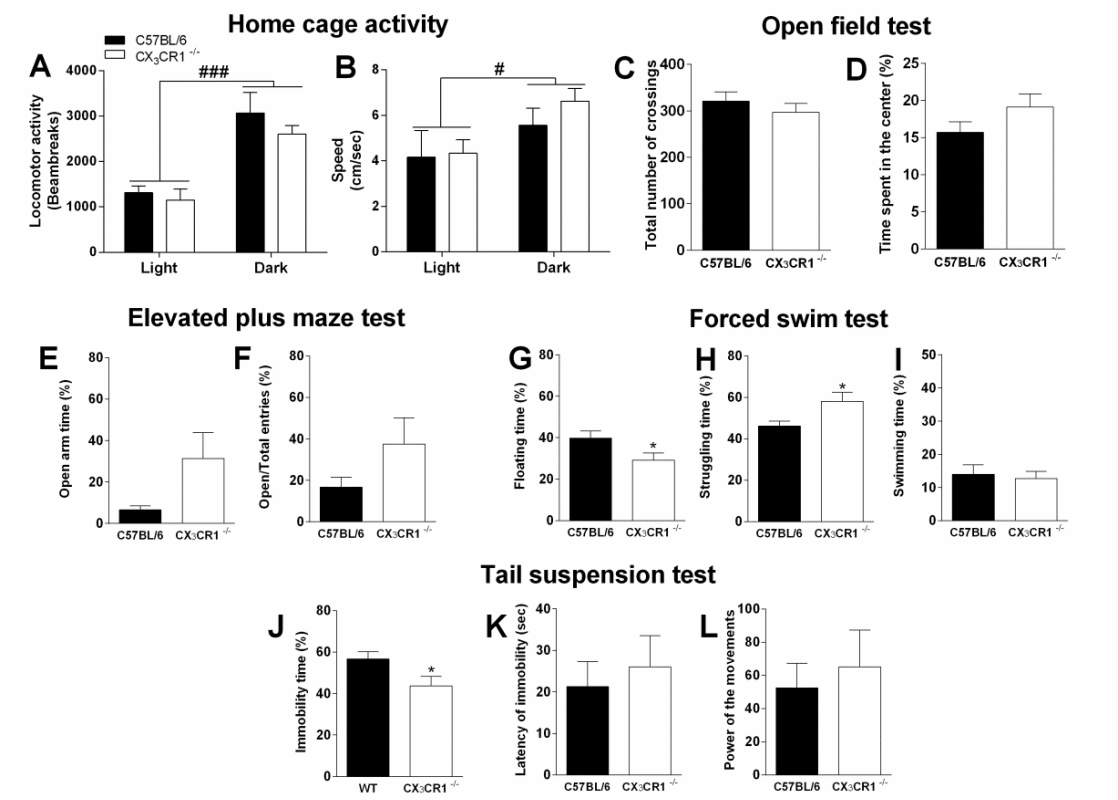

Fig.3. $CX_3CR1^{-/-}$ mice display active coping behavior in FST and in TST, but fractalkine receptor deficiency did not influence the locomotor activity of mice in their home cage and in open field test

(A) ***Home cage*** *locomotor* ***activity*** *and (B) the speed of the movements as recorded in TSE Phenomaster cages. Data were analyzed by two-way ANOVA (n = 8 per genotype). The main effect of day cycle: #p<0.05; ###p<0.001.* ***Open field test****: (C) The number of line crossings and (D) percentage of time spent in the central area (n = 8 per genotype).* ***Elevated plus maze***

test: *(E) The percentage of open arm time and (F) open arm preference (the ratio of open arm entries to the total entries) (n=7 per genotype).* ***Forced swim test (FST):*** *$CX_3CR1^{-/-}$ mice display active coping behavior in the forced swim test. The percentage of time spent with (G) floating, (H) struggling and (I) swimming (n=14/16 per genotype), *p<0.05 $CX_3CR1^{-/-}$ vs. C57BL/6 (Student's t-test).* ***Tail suspension test (TST):*** *(J) $CX_3CR1^{-/-}$ mice spent significantly less time immobile than C57BL/6 mice. (K) There was no significant difference between C57BL/6 and $CX_3CR1^{-/-}$ mice in either latency of immobility or (L) power of the movements (n=7/5 per genotype) *p<0.05 $CX_3CR1^{-/-}$ vs. C57BL/6 (Student's t-test). Bar graphs illustrate means ± SEM values [76].*

5.1.2. Acute psychological stress induced c-Fos expression in the PVN and the hypothalamo-pituitary-adrenocortical axis activity

Under basal, stress-free conditions, weak ***c-Fos labeling*** of a few scattered cells were detected in the PVN of both genotypes. Restraint stress-induced neuronal activation dramatically increased c-Fos counts 90 min after restraint stress [main effect of stress exposure: $F(1,11)=605.5$, $p<0.0001$] (Fig. 4A). The number of c-Fos positive cell nuclei within the PVN was significantly higher in $CX_3CR1^{-/-}$ mice after acute restraint, than in wild-type C57BL/6 mice. [Bonferroni's multiple comparisons test, $t(11)=3.193$, $p<0.05$] (Fig.4B).

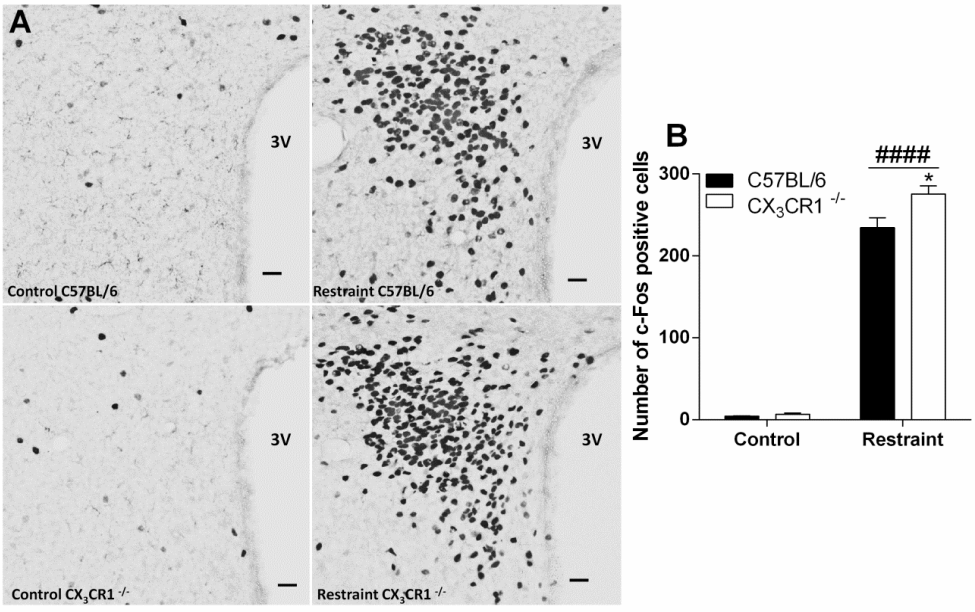

Fig.4. Acute restraint stress-induced neuronal activation in the paraventricular nucleus of the hypothalamus (PVN)

*(A) Representative photomicrographs showing c-Fos immunoreactive cell nuclei in the PVN in unstressed control and restrained, C57BL/6 and $CX_3CR1^{-/-}$ mice. 3V is the third ventricle on the right of the photomicrographs. Scale bar is 20 µm. (B) Number of c-Fos positive cell nuclei in the PVN of C57BL/6 and $CX_3CR1^{-/-}$ mice under non-stressed conditions and 90 min after restraint. Data are shown as mean values ± SEM (n=3/5 per group). Two-way ANOVA and Bonferroni post-hoc test. #### p<0.0001 the main effect of stress treatment; * p < 0.05 $CX_3CR1^{-/-}$ vs. C57BL/6 following restraint stress [76].*

Basal plasma ACTH levels in $CX_3CR1^{-/-}$ and wild-type mice did not differ significantly. Acute forced swim stress and restraint stress increased ACTH level [main effect of stress exposure: $F(2,17)=22.48$, $p<0.0001$]. Post hoc Bonferroni's multiple comparisons test showed significant difference between the genotypes after restraint stress [$t(17)=3.125$, $p<0.05$]: ACTH level rose higher in $CX_3CR1^{-/-}$ mice, than wild-type mice (Fig. 5A).

Under basal, non-stress conditions, plasma corticosterone level was elevated in $CX_3CR1^{-/-}$ animals compared to wild type mice. Both acute stressors (restraint and forced swim) resulted in a significant elevation of plasma corticosterone [main effect of stress exposure: $F(2,16)=128.4$, $p<0.0001$] and there was significant difference between genotypes [main effect of genotype: $F(1,16)=7.892$, $p=0.0126$], with the fractalkine receptor deficient mice reaching higher corticosterone levels than wild-type mice (Fig. 5B).

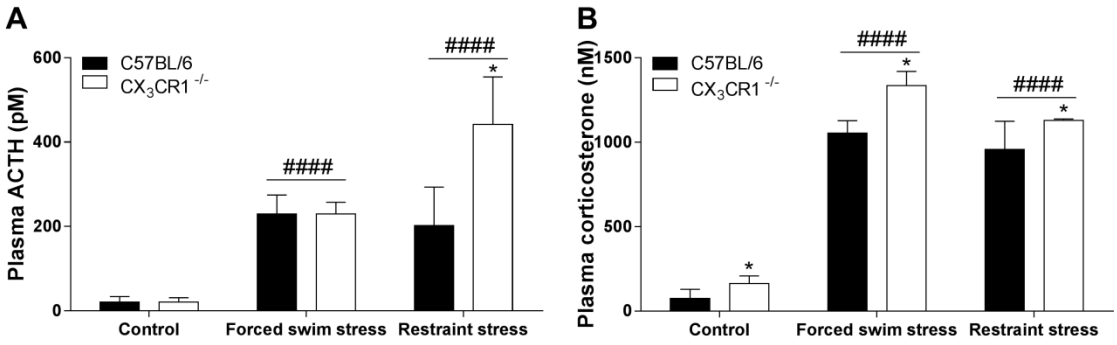

Fig.5. Effect of fractalkine receptor deficiency on basal and acute psychological stress-induced hypothalamo-pituitary-adrenal axis (HPA) activity

*(A) ACTH and (B) corticosterone plasma levels at basal, non-stress conditions and following forced swim and restraint stress in $CX_3CR1^{-/-}$ and wild-type mice. Mean values ± SEM. Data were analyzed by two-way ANOVA with Bonferrroni post hoc test (n=3/6 per group). The main effect of stress treatment: ####p<0.0001; main effect of genotype:*p<0.05 [76].*

5.1.3. Effect of acute restraint stress on the microglia in the paraventricular nucleus of the hypothalamus

Iba1 positive profiles were not uniformly distributed within the hypothalamic PVN region and they have been often found in close appositions with blood vessels. The analysis of Iba-1 positive cells in the PVN revealed only ramified and hyper-ramified microglia, and not reactive or phagocytic (Fig. 6A). Quantitative analysis of Iba1-immunreactivity from unstressed wild-type (C57BL/6) and fractalkine receptor deficient animals ($CX_3CR1^{-/-}$) revealed no significant differences in the density of Iba1+ microglia or in the area of Iba1+ profiles in the PVN area, although the nearest neighbor distance (NDD) was higher in the KO animals.

Following restraint stress, the area occupied by Iba1+ profiles was significantly decreased in the PVN of the fractalkine receptor deficient mice, but not in the wild-type [Bonferroni's multiple comparisons test, $t(12)=3.814$, $p<0.01$] (Fig. 6B). To reveal whether stress-induced decrease in Iba1-immunoreactive area in the PVN was related to changes in the number-,and/or distribution of microglia, the number of Iba1+ cells, and the nearest neighbor distance have also been measured and the spacing index was calculated. The number of Iba1 positive microglia decreased in stressed $CX_3CR1^{-/-}$ animals compared to C57BL/6 mice [Bonferroni's multiple comparisons test, $t(12)=2.746$, $p<0.05$] (Fig. 6C). The nearest neighbor distance did not change after stress, however was higher in $CX_3CR1^{-/-}$ mice compared to restrained C57BL/6 [main effect of genotype: $F(1,12)=6.673$, $p=0.0240$] (Fig. 6D). We also found a stress-related decrease of spacing index in restrained $CX_3CR1^{-/-}$ mice, [genotype × stress exposure interaction: $F(1,12) = 6,311$, $p = 0.0273$] (Fig. 6E), which was related to the decreased number of Iba1 positive microglia.

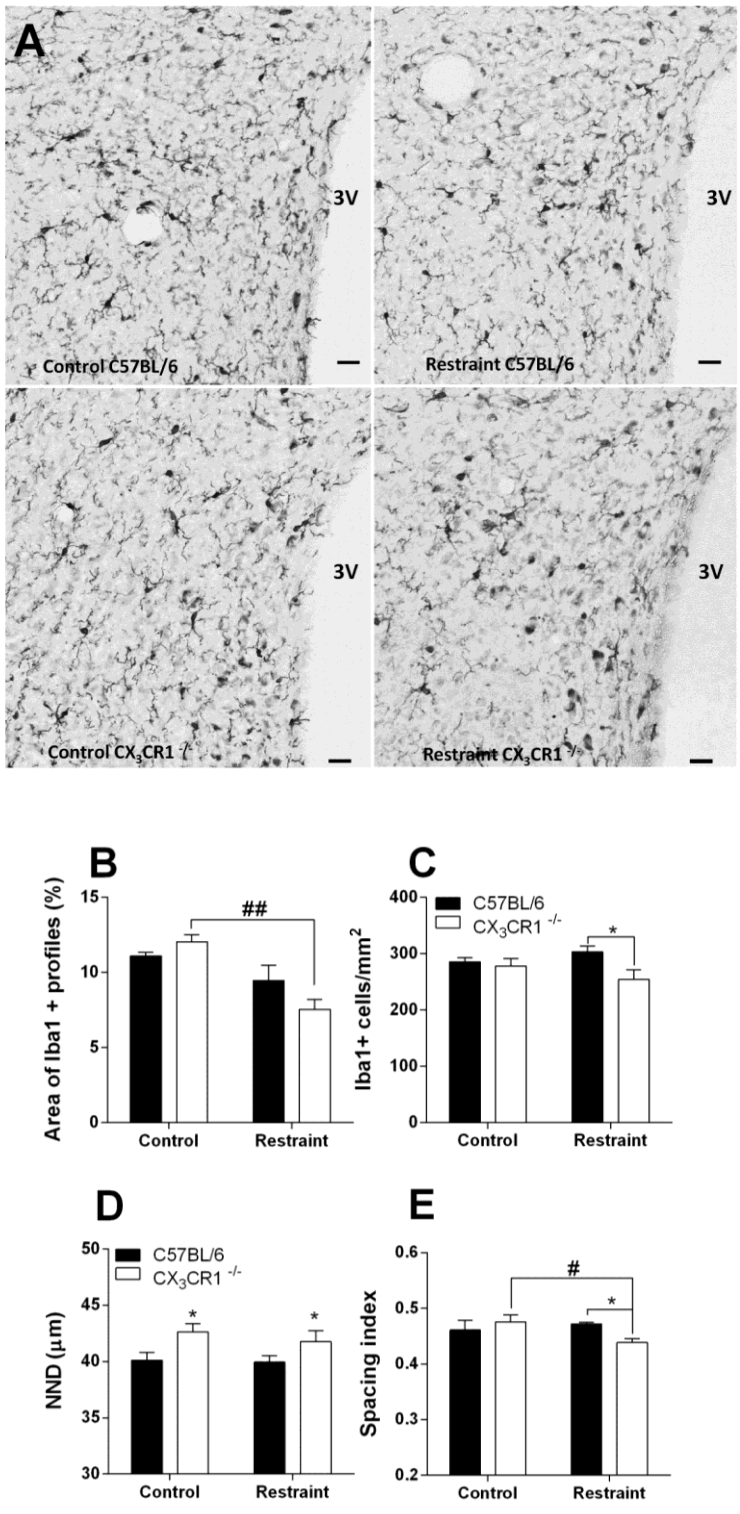

Fig.6. Effect of acute restraint stress on the microglia in the hypothalamus

(A) Representative images of paraventricular hypothalamic area showing Iba1 immunolabeled profiles. 3V is the third ventricle on the right. Scale bar is 20 µm. (B) Bar graphs showing mean values ± SEM the percentage (%) of the area occupied by Iba1+ profiles in control, non-

*stressed and stressed, C57BL/6 and $CX_3CR1^{-/-}$ mice. (C) Density of Iba1+ microglial cells in the paraventricular nucleus. (D) Average nearest neighbor distance (NND) as an average ± SEM calculated from individually labeled Iba1 positive microglia. (E) Spacing index (calculated as $NND^2 \times$Cell density). Two-way ANOVA with Bonferroni post hoc test (n=3/5 per group) #p<0.05, ##p<0.01 restraint stressed $CX_3CR1^{-/-}$ vs. control $CX_3CR1^{-/-}$; *p<0.05 $CX_3CR1^{-/-}$ vs. C57BL/6[76]*

5.2. Effects of "Two hit" chronic stress paradigm on fractalkine receptor deficient mice ($CX_3CR1^{-/-}$)

5.2.1. Body weight gain and behavioral responses

Body weight was measured just before chronic variable stress procedure (CVS) and at the end of CVS. Exposure to 3 weeks of CVS resulted in significant decrease in body weight gain in both genotypes [main effect of CVS: $F(1,35)=54.28$, $p<0.00001$] (Fig. 7A). No significant difference was found between wild-type and $CX_3CR1^{-/-}$ mice in body weight change [main effect of genotype: $F(1,35)=2.219$, $p>0.05$].

Anhedonia was tested in sucrose consumption test just before the CVS procedure and after 3-week CVS. Maternal separation (before CVS) had no effect on sucrose preference. However, pairwise comparisons of changes in sucrose preference revealed that CVS procedure resulted in a significant drop of sucrose preference in C57BL/6 mice but not in $CX_3CR1^{-/-}$ mice [Bonferroni's multiple comparisons test, $t(35)=2.426$, $p<0.05$] (Fig. 7D).

Anxiety-related behavior was tested on the ***elevated plus maze*** after the chronic variable stress procedure. MS+CVS did not affect the time spent on open arms [$F(1,12)=1.353$, $p>0.05$] (Fig. 7B), and the open arm preference (open/total entries %) [$F(1,12)=0.048$, $p>0.05$] (Fig.7C). The analysis did not identify any significant differences between genotypes as well.

In the ***open field test***, MS+CVS significantly decreased the time spent in central area [main effect of MS+CVS: $F(1,35)=4.76$, $p=0.0359$] (Fig. 7F), and increased the time in the corners [main effect of MS+CVS: $F(1,35)=4.67$, $p=0.0377$] (Fig. 7G). However, there was no difference between the genotypes. The total distance moved did not change in chronically stressed mice as compared to controls [main effect of MS+CVS: $F(1,35)=3.07$, $p>0.05$] (Fig. 7E).

DOI:10.14753/SE.2018.2148

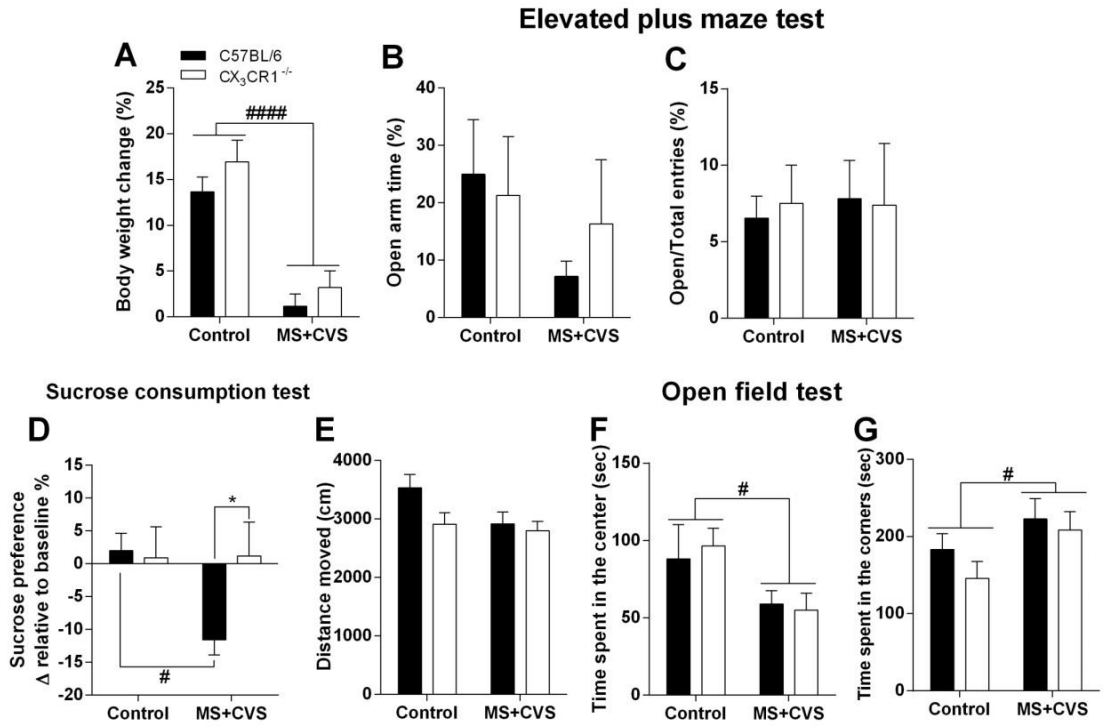

Fig.7. Effects of "Two hit" chronic stress paradigm on the body weight and behavioral parameters

C57BL/6 and $CX_3CR1^{-/-}$ mice were separated postnatally (PND 1-14) from their mothers then, as adults, were exposed to chronic variable stress (CVS) procedure for 3 weeks. Controls from each genotype were undisturbed.

*(A) Body weight change (as percentage of body weight gained during CVS/body weight before CVS). (B-C) Elevated plus maze test. (B) The percentage of open arm time and (C) open arm preference. (D) Sucrose preference (as the percentage of CVS-induced differences in sucrose preference relative to pre-CVS values). (E-G) Open field test. (E) Total distance moved, (F) time spent in the center, (G) time spent in the corners. Data are shown as mean values ± SEM (n=8/12 per group) and analyzed by two-way ANOVA. Main effect of chronic stress procedure: #p<0.05, ####p<0.0001. Main effect of genotype *p<0.05 [76].*

DOI:10.14753/SE.2018.2148

5.2.2. The effect of MS+CVS on the hypothalamo-pituitary-adrenocortical axis activity

Chronic stress (MS+CVS) resulted in a significant increase of relative ***adrenal weight*** in stressed mice of both genotypes compared to the values of the non-stressed control group [main effect of MS+CVS: $F(1,35)=23.44$, $p<0.0001$] (Fig. 8A). Chronic variable stress significantly decreased the relative ***thymus weight*** in $CX_3CR1^{-/-}$ mice [Bonferroni's multiple comparisons test, $t(16)=2.487$, $p<0.05$] (Fig. 8B), but not in C57BL/6 mice. However, MS+CVS procedure did not change ***plasma corticosterone*** levels significantly as measured at the end of the 3 week stress procedure [main effect of MS+CVS: $F(1,34)=0.02$, $p>0.05$] (Fig. 8C). ***Corticotrophin releasing hormone*** (CRH) ***mRNA*** expression was detected by in situ hybridization histochemistry in numerous regions of the mouse brain, mainly in the paraventricular nucleus of the hypothalamus (PVN), the central nucleus of the amygdala (CeA), the bed nucleus of the stria terminalis, the geniculate nucleus, the nucleus raphe magnus, the inferior olivary nucleus, and Barrington's nucleus. The PVN of the hypothalamus regulates the hypothalamic-pituitary-adrenal system, but extrahypothalamic CRH, especially in the limbic system, also play a role in the stress response [77]. In contrast to earlier findings [78], we did not measure increase in CRH mRNA expression in the PVN (Fig. 8D) and CeA (Fig. 8D) immediately after 3 weeks adult chronic variable stress either by in situ hybridization histochemistry, or by real-time quantitative PCR.

DOI:10.14753/SE.2018.2148

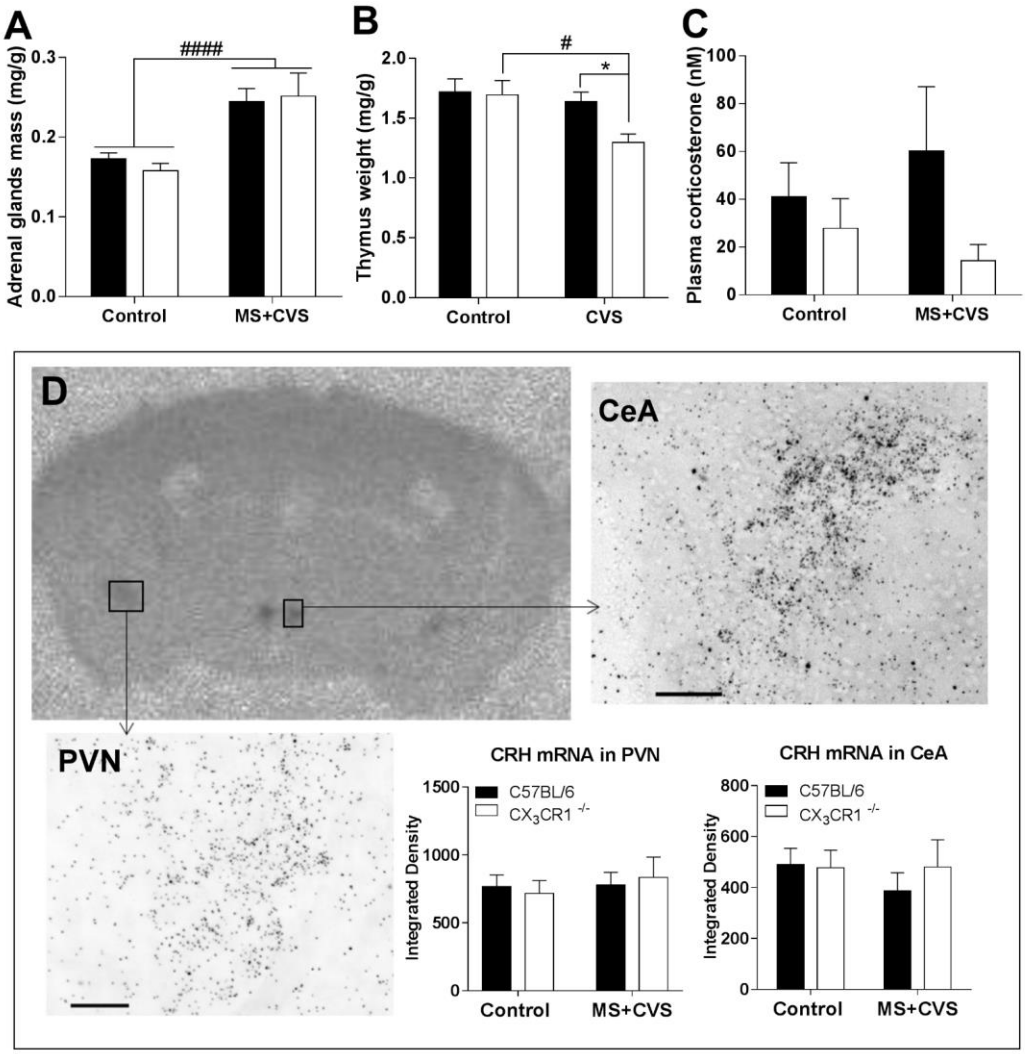

Fig.8. MS+CVS-induced HPA-axis activation

*(A) Normalized adrenal weight after exposure of MS+CVS (weight of the adrenal glands/ body weight). (B) Normalized thymus weight after exposure of MS+CVS (weight of the thymus/ body weight). (C) Plasma corticosterone concentration measured at the end of CVS procedure. (D) The quantitative analysis of CRH mRNA in situ hybridization in the PVN and in the CeA. Data are shown as mean values ± SEM and analyzed by two-way ANOVA. Main effect of chronic stress procedure: #p<0.05, ####p<0.0001. Main effect of genotype *p<0.05. Abbreviations: MS+CVS, maternal separation+ chronic variable stress [76]*

DOI:10.14753/SE.2018.2148

5.2.3. The effect of MS+CVS on the central and peripheral proinflammatory cytokine gene expression

The gene expression of proinflammatory cytokines within certain brain regions (hypothalamus, hippocampus, prefrontal cortex, amygdala) and in the liver were measured by RT-PCR after exposure to 3 weeks CVS or in non-stressed, control mice. MS+CVS led to enhancement in IL-1β mRNA expression in the hypothalamus [Bonferroni's multiple comparisons test, $t(9)=5.00$, $p<0.01$] and in the hippocampus [Bonferroni's multiple comparisons test, $t(10)=3.97$, $p=0.005$] solely in $CX_3CR1^{-/-}$ mice. Significant increase in IL-1α were detected in the hippocampus of $CX_3CR1^{-/-}$ mice [Bonferroni's multiple comparisons test, $t(10)=3.48$, $p<0.01$]. However, maternal separation and chronic variable stress induced significant IL-1α gene expression in the liver [main effect of MS+CVS: $F(1,10)=6.42$, $p<0.05$]. Significant down-regulation of IL-6 was found in the prefrontal cortex [main effect of genotype: $F(1,10)=5.07$, $p<0.05$], and in the liver [main effect of genotype: $F(1,11)=5.11$, $p<0.05$] of fractalkine receptor deficient mice (**Table 3**).

DOI:10.14753/SE.2018.2148

Table 3. MS+CVS-evoked proinflammatory cytokine gene expression pattern in the hypothalamus, hippocampus, prefrontal cortex, amygdala and in the liver.

*Measured by qRT-PCR results showing mean ± SEM values of fold change (FC, RQ) relative to non-stressed C57BL/6 mice. Red label: significant increase-, blue label: significant reduction of cytokine mRNA levels. N=3/5 per group, analyzed by two-way ANOVA. Main effect of chronic stress procedure: #p<0.05, ##p<0.01. Main effect of genotype *p<0.05, **p<0.01. Abbreviations: MS+CVS, maternal separation+ chronic variable stress; PFC, prefrontal cortex*

			Control		MS+CVS	
			C57BL/6	$CX_3CR1^{-/-}$	C57BL/6	$CX_3CR1^{-/-}$
IL-1a	Interleukin-1a	Hypotalamus	1	0.80±0.09	1.18±0.35	1.09±0.15
		Hippocampus	1	1.10±0.12	0.89±0.06	1.66±0.34 *
		PFC	1	0.88±0.04	1.06±0.05	1.14±0.15
		Amygdala	1	0.77±0.11	1.00±0.15	0.85±0.07
		Liver	1	0.81±0.17	1.58±0.36 #	1.47±0.12 #
IL-1b	Interleukin-1b	Hypotalamus	1	0.59±0.07	1.69±0.10	2.93±0.67 *; ##
		Hippocampus	1	0.84±0.02	0.87±0.04	1.48±0.14 **; ##
		PFC	1	1.34±0.37	0.69±0.26	0.80±0.16
		Amygdala	1	0.48±0.16	0.73±0.06	0.78±0.12
		Liver	1	0.88±0.04	1.31±0.34	1.42±0.40
IL-6	Interleukin-6	Hypotalamus	1	0.71±0.25	0.57±0.25	0.82±0.25
		Hippocampus	1	0.50±0.02	0.84±0.16	0.87±0.27
		PFC	1	0.18±0.02 *	0.76±0.30	0.37±0.16 *
		Amygdala	1	0.76±0.02	0.92±0.06	1.14±0.12
		Liver	1	0.43±0.17 *	0.98±0.18	0.67±0.08 *

DOI:10.14753/SE.2018.2148

5.2.4. Effects of MS+CVS on the microglia in the paraventricular nucleus

Iba1 positive cells were not uniformly distributed within the hypothalamic paraventricular nucleus: cells were more often visualized medially, closed to the wall of the third ventricle (Fig. 9A). Quantitative analysis of distribution markers (NND and spacing index) did not reveal significant differences between genotypes [main effect of genotype: $F(1,11)=1.606$, $p>0.05$] (Fig. 9).

In animals exposed to chronic stress, the number of Iba-1 positive cells decreased compared to non-stressed controls [main effect of MS+CVS: $F(1,11)=5.899$, $p=0.0335$] (Fig. 9C), while the area of Iba1+ profiles (Fig. 9B) and the spacing index in the PVN remained unchanged. We observed a significant genotype-related increase in the distance of the nearest neighbor microglia (NND) following MS+CVS in the PVN [Bonferroni's multiple comparisons test, $t(11)=2.673$, $p=0.0433$] (Fig. 9D), which could be explained by the decreased density of microglia in the PVN of fractalkine receptor deficient mice.

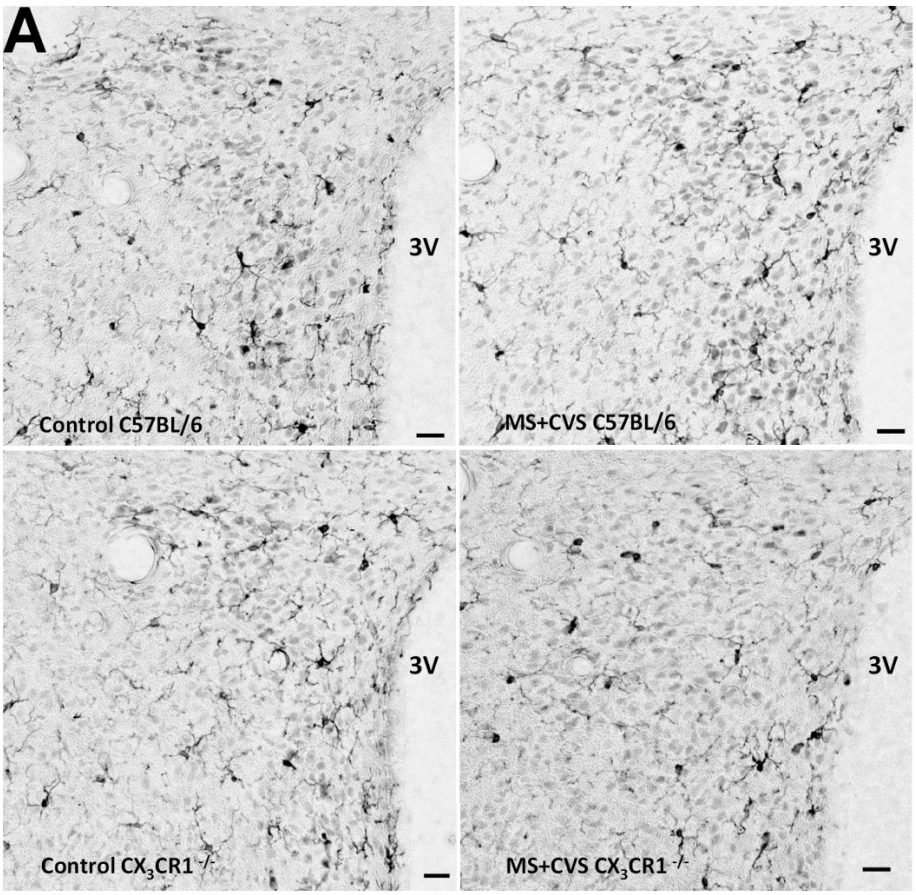

DOI:10.14753/SE.2018.2148

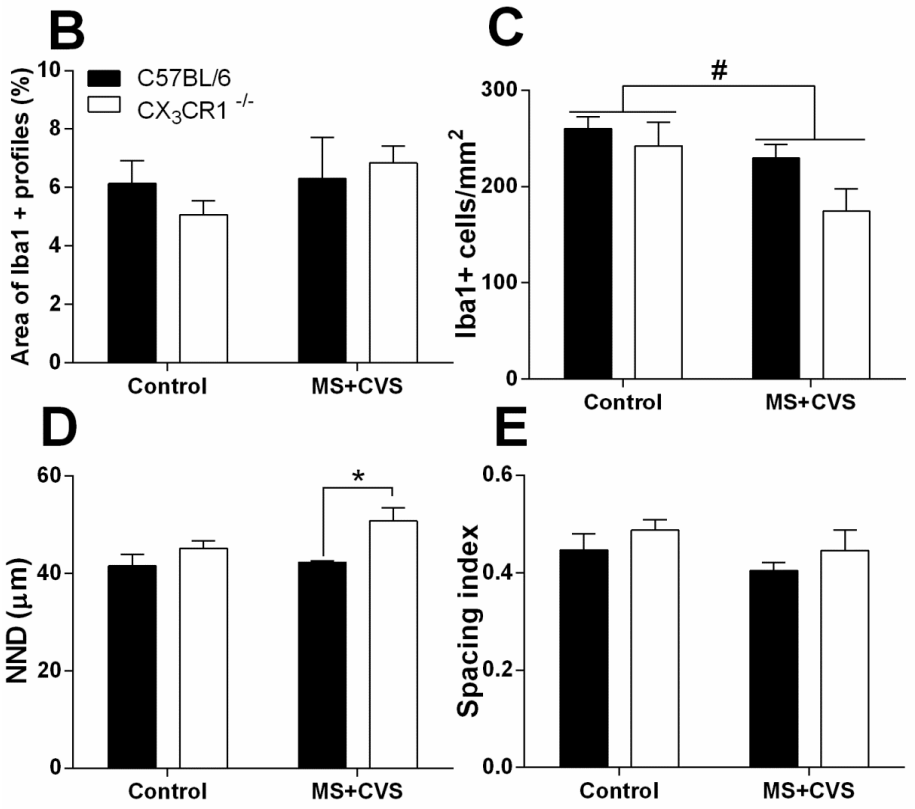

Fig.9. Effects of MS+CVS on the hypothalamic microglia

*(A) Representative images of paraventricular hypothalamic area showing Iba1 immunolabeled profiles. 3V is the third ventricle on the right. Scale bar is 20 µm. (B) the percentage (%) of the area occupied by Iba1+ profiles in control, non-stressed and chronic stressed, C57BL/6 and $CX_3CR1^{-/-}$ mice. (C) Density of Iba1+ microglial cells in the paraventricular nucleus. (D) Average nearest neighbor distance (NND) as an average ± SEM calculated from individually labeled Iba1 positive microglia. (E) Spacing index (calculated as $NND^2 \times$Cell density). Bar graphs are showing mean values ± SEM (n=3/4 per group), two-way ANOVA with Bonferroni post hoc test. #p<0.05 main effect of MS+CVS; *p<0.05 $CX_3CR1^{-/-}$ vs. C57BL/6. Abbreviations: MS+CVS, maternal separation+ chronic variable stress [76]*

5.3. Effects of acute physiological challenge on $CX_3CR1^{-/-}$ mice

5.3.1. Effects of fasting and insulin-induced hypoglycemia on metabolic parameters

Fractalkine receptor deficiency did not affect the baseline feeding behavior (Fig. 10A), body weight (Fig. 10B), respiratory exchange ratio (Fig. 10C, D), fatty acid oxidation (Fig. 10E), and locomotor activity (Fig. 10F) under standard conditions. However, significant difference was detected between the genotypes in the energy expenditure (Fig. 10G,H) [Bonferroni's multiple comparisons test, $t(124)=3.321$, $p=0.01$], increased energy expenditure was observed in fractalkine receptor deficient mice ($CX_3CR1^{-/-}$) [76].

The overnight fasting significantly decreased body weight regardless of genotype [main effect of fasting: $F(1,14)=90.47$, $p<0.0001$] (Fig. 10B). Fasted mice exhibited significant decrease in energy expenditure (Fig. 10G,H) [main effect of fasting: $F(1,124)=361.7$, $p<0.0001$] and locomotor activity (Fig. 10F) in the active phase of the circadian rhythm. The overnight fasting resulted in a significant decrease in the respiratory exchange ratio (RER) [main effect of fasting: $F(1,28)=620.5$, $p<0.0001$] (Fig. 10C,D) compared to the fed state. Based on the respiratory exchange ratio (RER) values, fasted mice used fatty acids as the primary source of fuel ($RQ=0.68\pm0.028$). These values are consistent with the calculated parameter, the fatty acid oxidation (%). Fatty acid oxidation enhanced significantly during starvation in both genotypes (Fig. 10E) [main effect of fasting: $F(1,124)=3200$, $p<0.0001$].

Immediately after insulin injection, RER transiently increased indicating cellular uptake and metabolism of glucose, showed peak at 30 min ($RQ=0.74$) and declined the fasted baseline level by 180 min (Fig. 11A), while the locomotor activity displayed a maximum at 15 min and minimum at 120 min. Following insulin-induced hypoglycemia the $CX_3CR1^{-/-}$ mice presented more active locomotor behavior than C57BL/6 mice (Fig. 11D) [$t(12)=2.79$, $p=0.016$]. The energy expenditure remained approximately unchanged during the 180 min period of hypoglycemia (Fig. 11C). No significant difference was detected between the genotypes in RER, energy expenditure and fatty acid oxidation (Fig. 11B) during insulin-induced hypoglycemia.

DOI:10.14753/SE.2018.2148

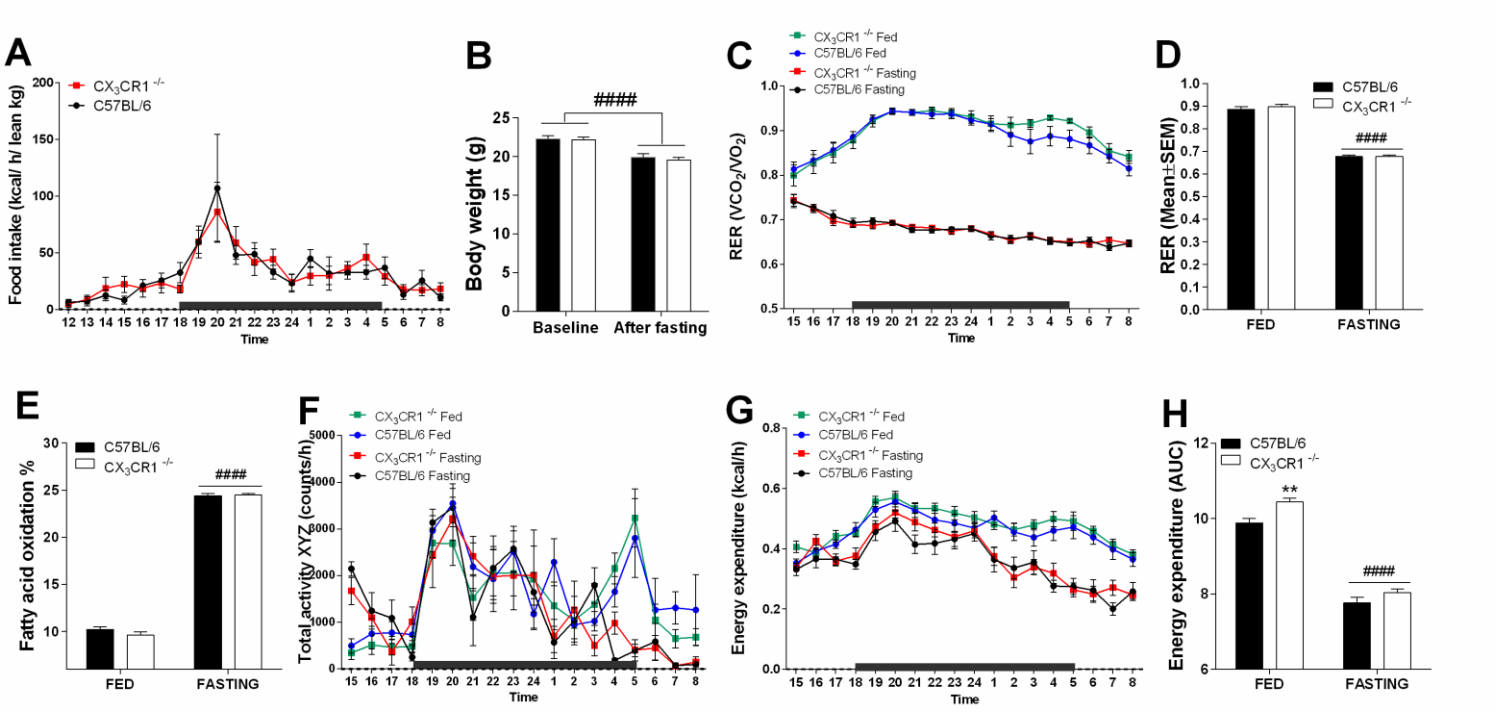

Fig.10. Metabolic phenotype of fractalkine receptor deficient mice ($CX_3CR1^{-/-}$) during control, fed conditions and overnight fasting

*(A) Food intake, (C,D) respiratory exchange ratio (RER), (E) fatty acid oxidation %, (F) total activity and (G,H) energy expenditure data were automatically collected from individual mice (n = 8 per group) at 10 minute intervals over a 72 hour period in TSE Phenomaster cages. Statistical analysis was performed using two-way ANOVA.(B) The body weight was measured before and after overnight fasting, analyzed by two-way ANOVA with repeated measurement. Mean values ± SEM are shown. The main effect of fasting: ####p<0.0001; the main effect of genotype: **p<0.01. Abbreviation: AUC, area under the curve*

DOI:10.14753/SE.2018.2148

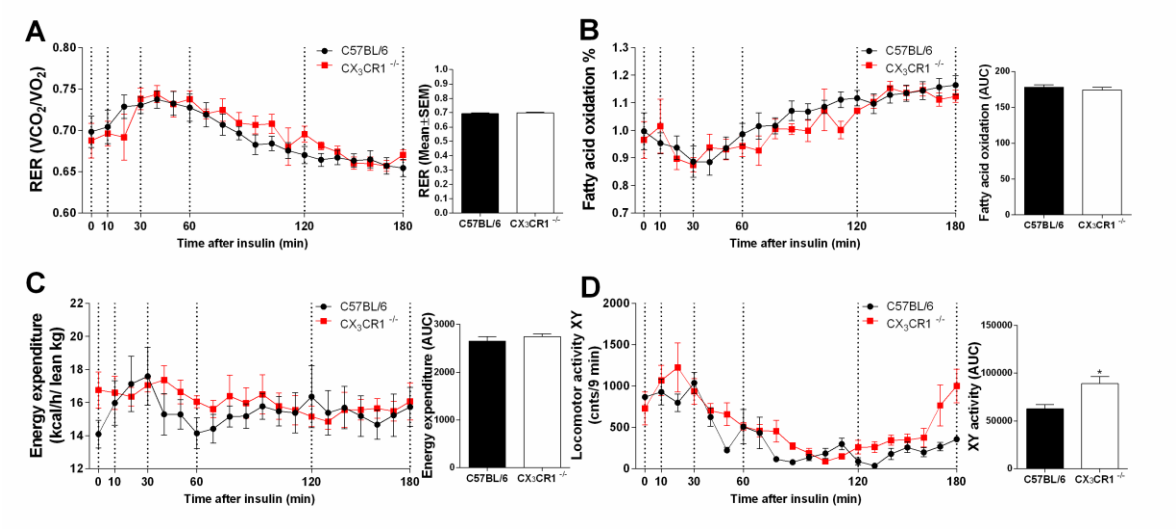

Fig.11. Effect of ip. insulin administration after overnight fasting on the metabolic parameters

(A) Respiratory exchange ratio (RER), (B) fatty acid oxidation %, (C) energy expenditure, and (D) locomotor activity were measured at 10 minute intervals over a 180 min period in TSE Phenomaster cages following ip. insulin administration. Mean values ± SEM are represented. p<0.05 C57BL/6 vs. $CX_3CR1^{-/-}$ mice (Student's t-test). Abbreviation: AUC, area under the curve*

DOI:10.14753/SE.2018.2148

5.3.2. Fractalkine receptor (CX_3CR1) deficient mice mount increased counter-regulatory responses to neuroglycopenia and insulin-induced hypoglycemia

Systemic administration of 2-deoxy-D-glucose (2-DG) results in counter-regulatory increase in blood glucose levels in non-fasted rodents. Two-way ANOVA revealed significant treatment [$F(1, 11) = 80.19$, $p<0.0001$] and genotype effect [$F(1, 11) = 38.83$, $p<0.0001$] (Fig. 12A).

Insulin injection to fasted C57BL/6 mice resulted in severe hypoglycemia with blood glucose levels 2,12 ± 0,11 mM) compared to fed (8,88 ± 0,24 mM) or fasted (4,34 ± 0,12 mM) controls at 60 min post-injection. $CX_3CR1^{-/-}$ mice do not develop hypoglycemia in response insulin (blood glucose in C57BL/6: 2,02 ± 0,13 mM vs $CX_3CR1^{-/-}$ mice: 3,58 ± 0,45 mM; t= 2,54, df=8; p=0.017) (Fig. 12B).

Hypoglycemia evokes a strict coordinated sequence of counter-regulatory hormone responses to restore normoglycemia. My experiments were in line with our previous results [79], acute insulin-induced hypoglycemic stress caused HPA-axis activation (Fig.12.). Real-time quantitative PCR measurement revealed that insulin-induced hypoglycemia stimulated CRH mRNA expression in the hypothalamus [main effect of Fast+INS: $F(1,8)=96.04$, $p<0.0001$]. Furthermore, CRH mRNA expression in the hypothalamus was significantly higher in $CX_3CR1^{-/-}$ mice than wild-type mice in control conditions, and after insulin treatment [main effect of genotype: $F(1,8)=228.3$, $p<0.0001$] (Fig. 12C). Corticosterone level rose significantly 1 hour after ip. insulin injection in both genotypes [main effect of Fast+INS: $F(1,11)=200.1$, $p<0.0001$] (Fig. 12E), but the elevation of plasma ACTH was not significant [main effect of Fast+INS: $F(1,11)=2.558$, $p=0.14$] (Fig. 12D). Hypoglycemia induced increase in sympatho-adrenal response following 1 h insulin administration. Plasma epinephrine level elevated in $CX_3CR1^{-/-}$ mice significantly after insulin injection [Bonferroni's multiple comparisons test, $t(10)=2.75$, $p<0.05$] (Fig. 12F). There was a significant difference in plasma norepinephrine levels between the two genotypes after insulin-induced hypoglycemia [Bonferroni's multiple comparisons test, $t(7)=3.5$, $p<0.05$] (Fig. 12G).

DOI:10.14753/SE.2018.2148

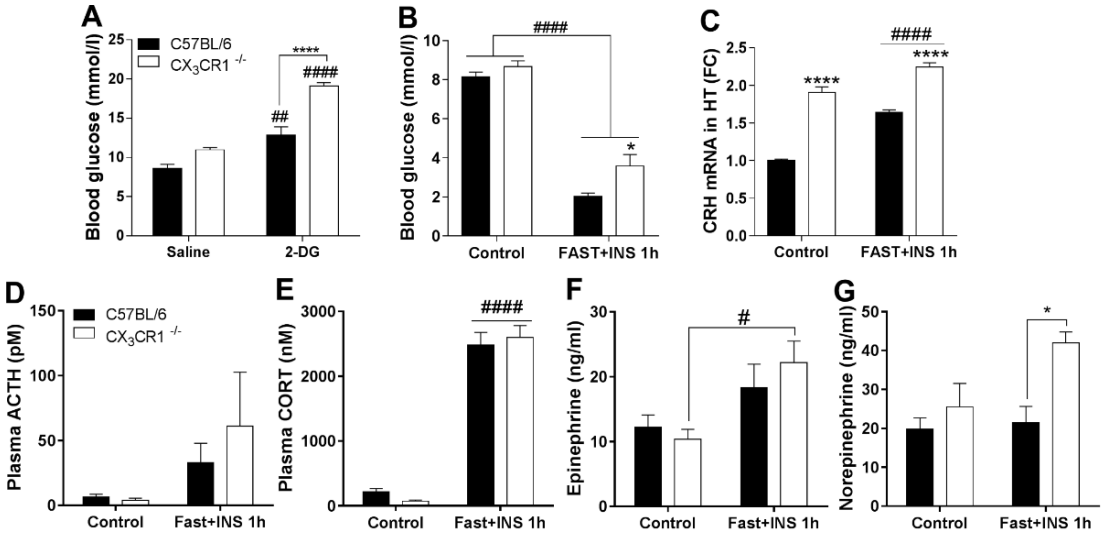

Fig.12. Fractalkine receptor (CX_3CR1) deficient mice mount increased counter-regulatory responses to neuroglycopenia and insulin-induced hypoglycemia

*(A) Blood glucose levels after 1 hour ip. 2-DG administration. (B) Blood glucose levels after overnight fasting and 1 hour ip. insulin injection. (C) Corticotropin-releasing hormone (CRH) mRNA levels in the hypothalamus. (D) Plasma ACTH, (E) corticosterone, (F) epinephrine and (G) norepinephrine levels. Statistical analysis was performed using two-way ANOVA. Mean values ± SEM are shown. The main effect of Fast+INS: #p<0.05, ##p<0.01, ####p<0.0001; the main effect of genotype: *p<0.05, ****p<0.0001. Abbreviation: 2-DG, 2-deoxy-glucose*

DOI:10.14753/SE.2018.2148

5.3.3. Hypoglycemia selectively activates orexigenic neurons in the hypothalamic arcuate nucleus

Hypoglycemia induced by peripheral administration of insulin dramatically enhanced c-Fos immunoreactivity in the hypothalamic arcuate nucleus [main effect of Fast+INS: $F(1,8)=42.38$, $p<0.001$] (Fig. 13B). Co-localization of NPY or POMC mRNA with c-Fos protein in the medial basal hypothalamus revealed selective activation of orexigenic NPY neurons (Fig. 13A). The relative expression of NPY mRNA, as measured by RT-PCR, increased significantly [$F(1,12)=52.28$, $p<0.0001$], and AgRP mRNA elevated two fold as well [$F(1,12)=51.31$, $p<0.0001$]. Furthermore, $CX_3CR1^{-/-}$ mice displayed significantly higher NPY mRNA [Bonferroni's multiple comparisons test, $t(12)=4.301$, $p<0.001$] and AgRP mRNA response to insulin-induced hypoglycemia than wild-type animals [Bonferroni's multiple comparisons test, $t(12)=4.171$, $p<0.001$]. Hypothalamic POMC expression in the arcuate nucleus remained unchanged in both genotypes (Fig. 13D).

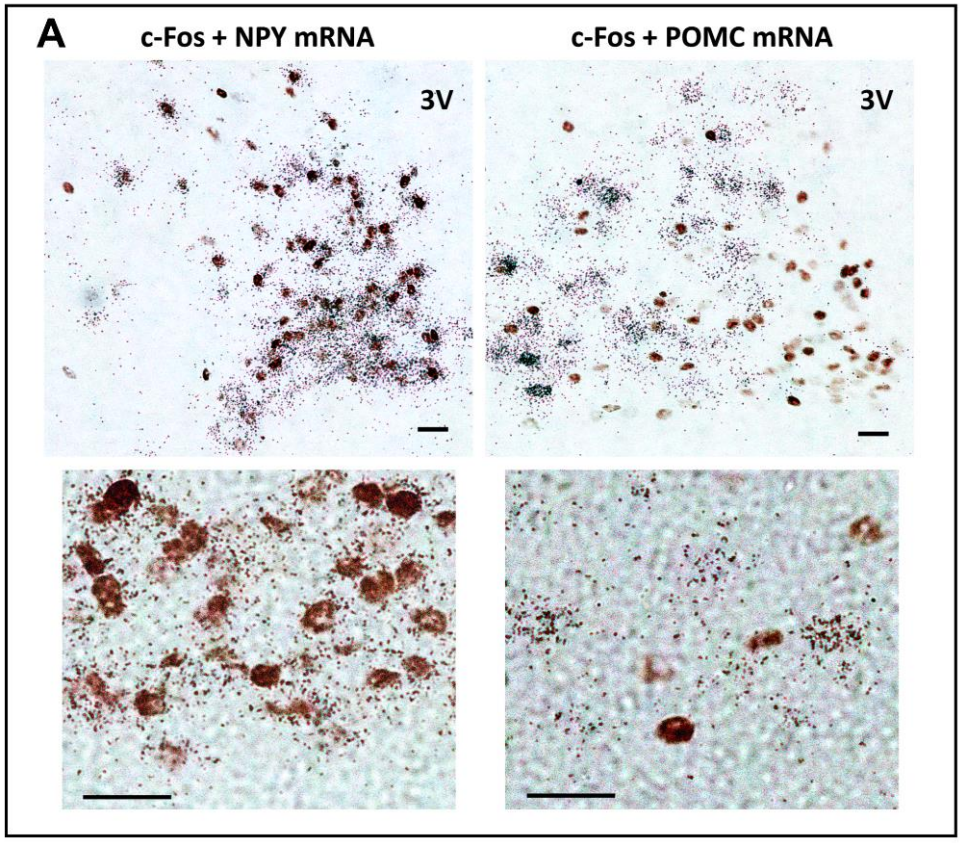

DOI:10.14753/SE.2018.2148

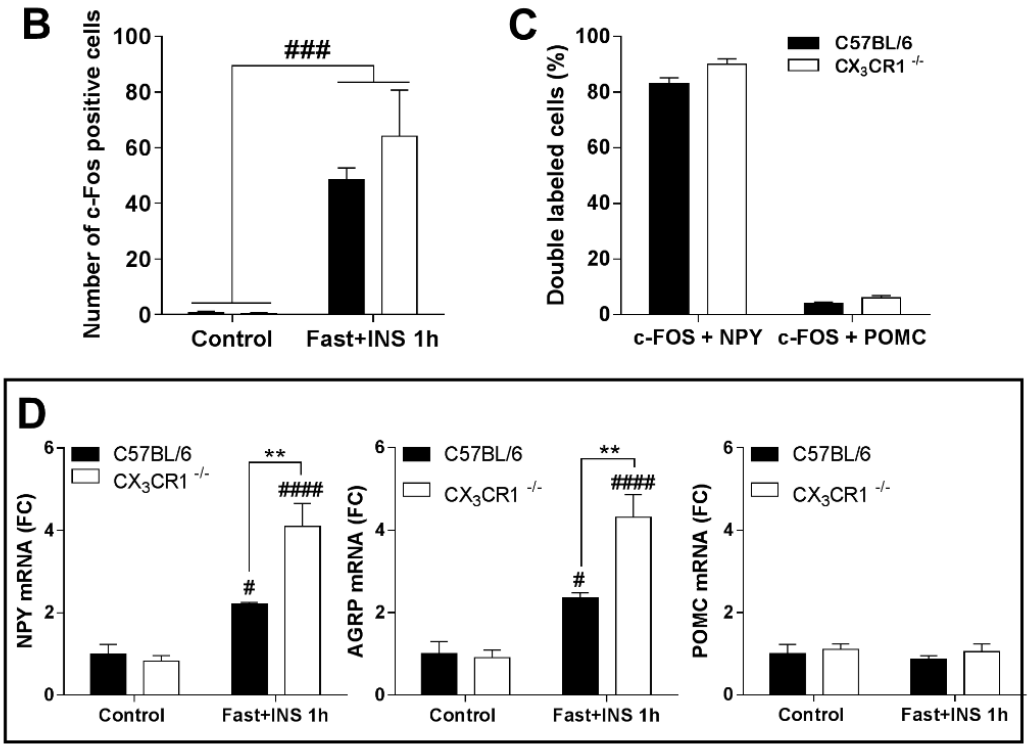

Fig.13. Hypoglycemia selectively activates NPY expressing, orexigenic neurons in the hypothalamic arcuate nucleus.

*(A) Combined c-Fos immunocytochemistry and NPY or POMC mRNA in situ hybridization demonstrates c-Fos positive cell nuclei (brown) in NPY or POMC mRNA expressing neurons (black autoradiographic grains) in the arcuate nucleus of hypothalamus following insulin-induced hypoglycemia. 3V is the third ventricle on the right. Scale bar is 20 µm. (B) Quantitative analysis of c-Fos immunohistochemistry in the arcuate nucleus of C57BL/6 and $CX_3CR1^{-/-}$ mice under control condition and 1 hour after ip. insulin injection. (C) Quantitative analysis of co-localization of c-Fos with NPY mRNA or POMC mRNA in the arcuate nucleus (ARC) of control and insulin-treated C57BL/6 and $CX_3CR1^{-/-}$ mice. (D) Relative quantities of NPY, AGRP and POMC mRNAs in the ARC of wild-type and fractalkine receptor deficient mice under control conditions or after insulin-injection. n= 4 per group, Two-way ANOVA with Bonferroni post hoc test. The main effect of Fast+INS: #p<0.05, ####p<0.0001; $CX_3CR1^{-/-}$ vs. C57BL/6: **p<0.01*

DOI:10.14753/SE.2018.2148

5.3.4. Hypoglycemia results in morphological changes in microglia selectively in the hypothalamic arcuate nucleus

The morphology of ionized calcium-binding adaptor molecule 1 (Iba1) + cells in the arcuate nucleus of hypoglycemic mice were visually different from controls. In fed and fasted control animals, Iba-1 immunostaining revealed predominantly resting form of microglia with moderate perisomatic immunoreactivity and fine branching processes. By contrast, in the hypothalamus of hypoglycemic animals, microglia displayed activated phenotype with thickened branches and increased Iba1-immunoreactivity (Fig. 14A). Furthermore, these "thickened" microglial cells were concentrated around c-Fos+ activated neuron population in the rostral and medial portion of the arcuate nucleus (ARC). Quantitative analysis showed that the area of Iba1+ profiles elevated significantly after insulin injection in the ARC [main effect of Fast+INS: $F(1,8)=7.839$, $p=0.023$] (Fig. 14B). Furthermore, in the rostral ARC there was a significant difference between genotypes in the area of Iba1+ profiles after insulin-induced hypoglycemia [Bonferroni's multiple comparisons test, $t(6)=4.95$, $p<0.01$] (Fig. 14C). In addition, the density of Iba1+ microglial cells increased significantly in the hypoglycemic mice regardless of genotype [main effect of Fast+INS: $F(1,7)=22.27$, $p<0.01$] (Fig. 14D). In hypoglycemic mice, the nearest neighbor distance [main effect of Fast+INS: $F(1,7)=35.23$, $p<0.001$] (Fig. 14F) and the spacing index decreased significantly in the ARC [main effect of Fast+INS: $F(1,7)=5.782$, $p=0.047$] (Fig. 14G). These parameters indicate that microglial cells were located nearer to each other. Morphological analysis of microglia population in the arcuate nucleus revealed significant effect of insulin treatment on the processes' density of microglial cells [$F(1, 8) = 26.77$, $p<0.001$] (Fig. 14E).

DOI:10.14753/SE.2018.2148

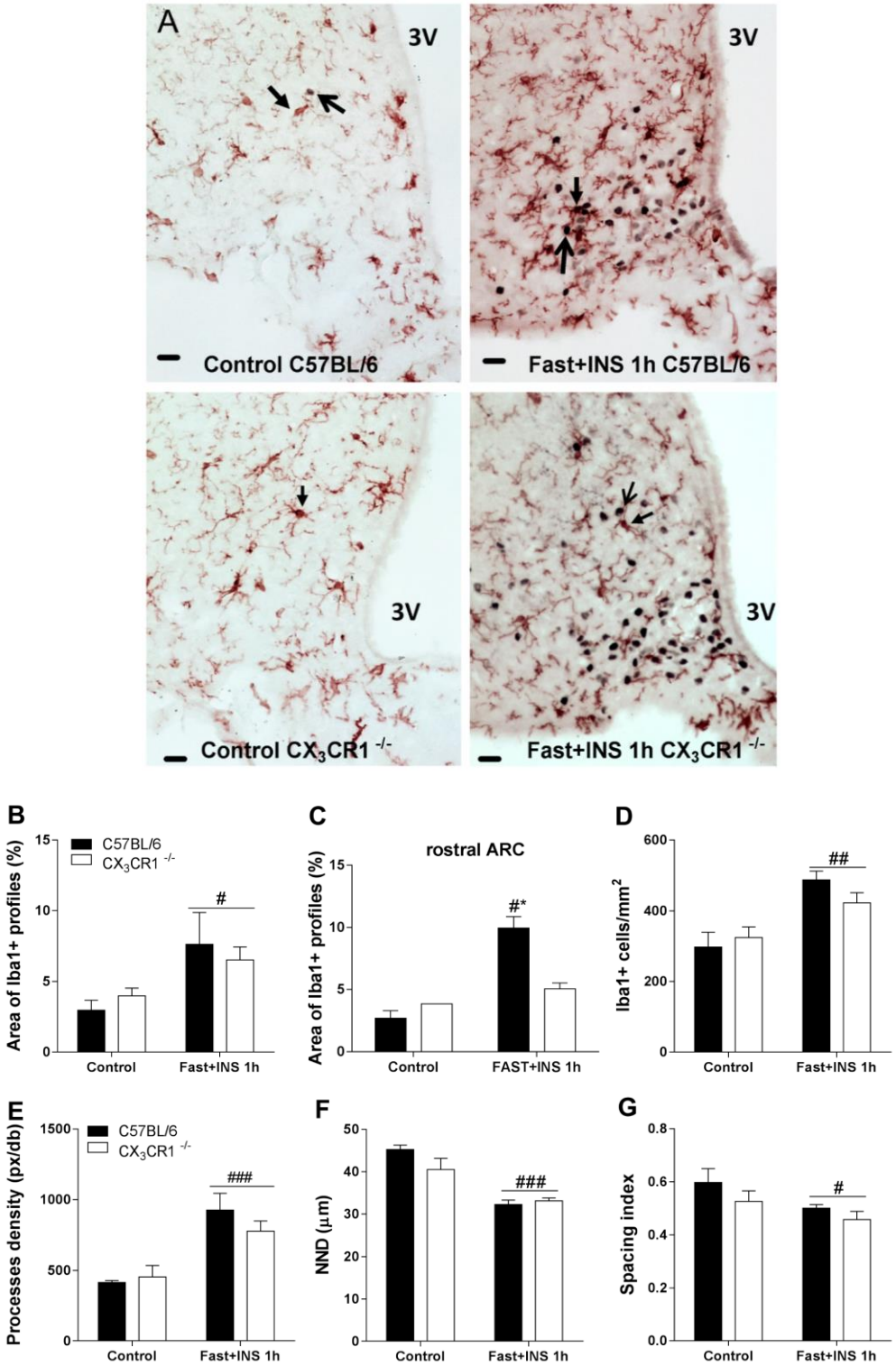

Fig.14. Effects of insulin-induced hypoglycemia on the microglia in the hypothalamic arcuate nucleus

(A) Representative photomicrographs of Iba1 (brown) and c-Fos (black) double immunostaining within the arcuate nucleus of the hypothalamus (ARC). 3V is the third ventricle

*on the right. Scale bars indicate 20 µm. (B) The percentage (%) of the area occupied by Iba1+ profiles in control, and insulin-induced hypoglycemia following fasting, C57BL/6 and CX3CR1 -/- mice in the ARC (between bregma -1.22 and -1.94). (C) The percentage (%) of the area occupied by Iba1+ profiles in the rostral part of ARC (between bregma -1.22 and -1.4). (D) Density of Iba1+ microglial cells in the ARC. (E) The processes density as a morphological index of Iba1 + microglia in the ARC. (F) Average nearest neighbor distance (NND) as an average ± SEM calculated from individually labeled Iba1 positive microglia. (G) Spacing index (calculated as NND2×Cell density). Bar graphs are showing mean values ± SEM (n= 3 per group). Two-way ANOVA with Bonferroni post hoc test. The main effect of Fast+INS: #p<0.05, ##p<0.01, ###p<0.001; CX3CR1 -/- vs. C57BL/6: *p<0.05.*

Insulin-induced hypoglycemia resulted remarkable c-Fos expression in the paraventricular nucleus of the hypothalamus as well [main effect of Fast+INS: $F(1,8)=370.2$, $p<0.0001$] (Fig. 15A,B). However, qualitative and quantitative analysis of Iba1 positive profiles in the hypothalamic paraventricular nucleus did not reveal any signs of microglia activation (Fig. 15C), suggesting that the hypoglycemia-induced microglia activation was specific for the arcuate nucleus.

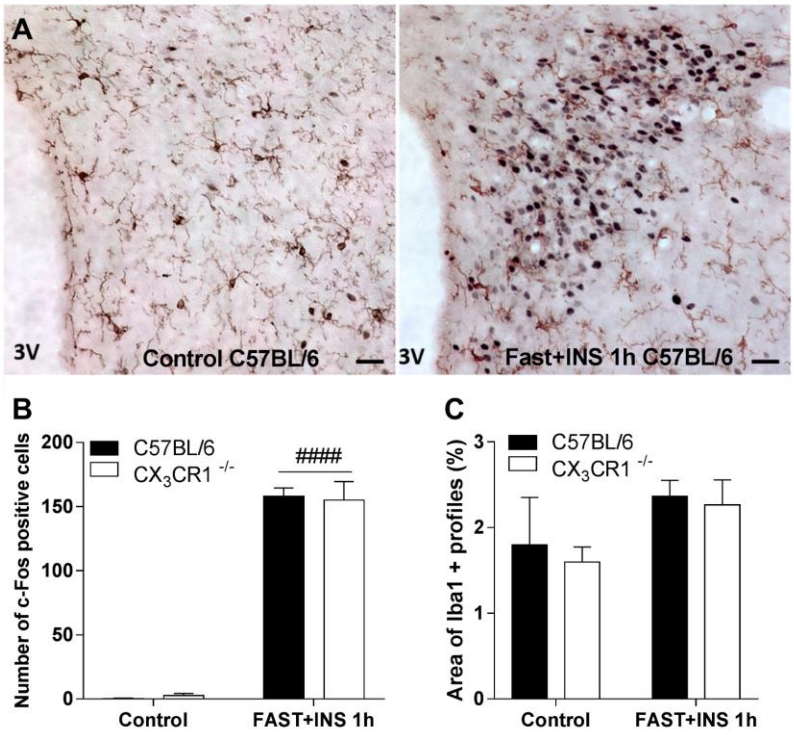

Fig.15. c-Fos and Iba-1 immunreactivity in the paraventricular nucleus of the hypothalamus after insulin-induced hypoglycemia

(A) Representative images of Iba1 (brown cells) and c-Fos (black nuclei) double immunostaining within the paraventricular nucleus of the hypothalamus (PVN) (between bregma - 0.58 and -0.94). 3V is the third ventricle on the right. Scale bars indicate 20 µm. (B) Quantitative analysis of c-Fos + neurons in the PVN under control condition and 1 hour after ip. insulin injection. (C) The percentage (%) of the area occupied by Iba1+ profiles in the PVN. Diagrams are showing mean values ± SEM. Two-way ANOVA. The main effect of Fast+INS: ####p<0.001

5.3.5. Activated microglia make close appositions with c-Fos positive neurons in the arcuate nucleus

There was a certain trend toward significance between the two genotypes in the distance between c-Fos+ neurons and the Iba1+ microglia [t(4)=2.256, p=0.087] (Fig. 16A). Microglia with functioning fractalkine receptor were closer to hypoglycemia-activated neurons in the ARC than those microglia with impaired fractalkine receptor. Confocal imaging of triple fluorescent-labeled material (GFP –microglia; c-Fos –activated profiles and neurofilament H (SMI32) – neuronal cell bodies) revealed close apposition of GFP-positive microglia (in $CX_3CR1^{+/-}$ mice) and hypoglycemia-activated neurons (Fig. 16B).

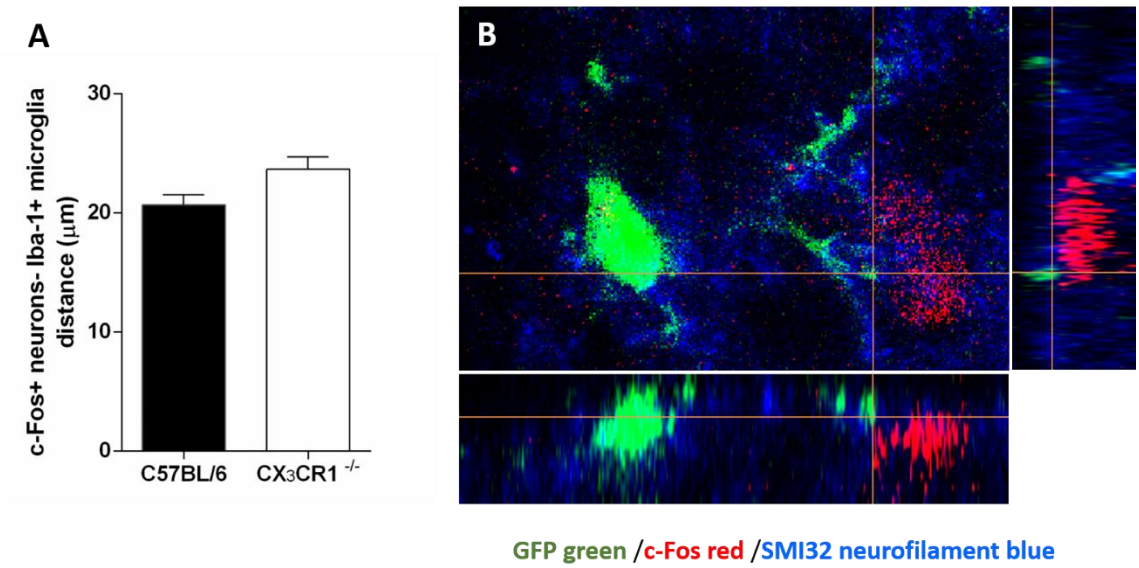

Fig.16. Microglial processes make close appositions with activated neurons in the arcuate nucleus

(A) Average distance between c-Fos+ neurons and the nearest Iba1+ microglia in the ARC (between bregma -1.22 and -1.94) after insulin-induced hypoglycemia. Data are derived from the quantitative analysis of c-Fos and Iba1 double immunostained sections. Bar graph shows mean values ± SEM. (B) Confocal imaging of triple fluorescent-labeled material (GFP – microglia; c-Fos –activated profiles and neurofilament H (SMI32) – neuronal cell bodies) in the ARC of $CX_3CR1^{+/-}$ mice.

5.4. Minocycline attenuates microglia activation and results in less severe hypoglycemic response to insulin

Next, we investigated whether inhibition of microglia affects hypoglycemic response to insulin. Icv. infusion of microglia blocker minocycline attenuated insulin-induced microglia activation in the hypothalamus. As shown in Figure 17., the area of Iba1+ profiles decreased significantly in the arcuate nucleus in minocycline pretreated and insulin-induced hypoglycemic mice compared to control animals [t(6)=4.33, p=0.005] (Fig. 17E). The cell body/cell size ratio was higher in the arcuate nucleus of minocycline pretreated, insulin injected mice compared to vehicle pretreated controls [t(6)=3.68, p=0.01] (Fig. 17G), and simultaneous decrease in processes density was measured [t(6)=3.25, p=0.018] (Fig. 17H). Microglia inhibition by minocycline resulted in a 36% higher blood glucose level 1h after insulin [t(8)=2.867, p=0.021] (Fig. 17A), which was associated with an elevation of plasma adrenaline and noradrenaline concentration, compared to vehicle-pretreated, insulin-injected controls (Fig. 17B,C).

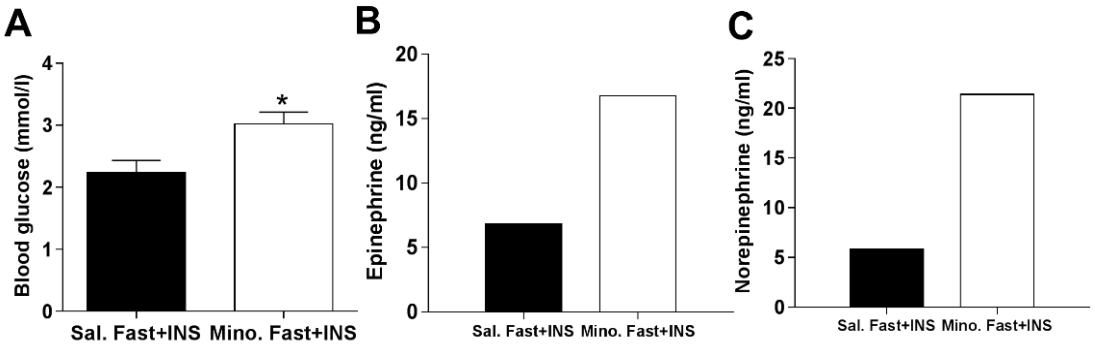

DOI:10.14753/SE.2018.2148

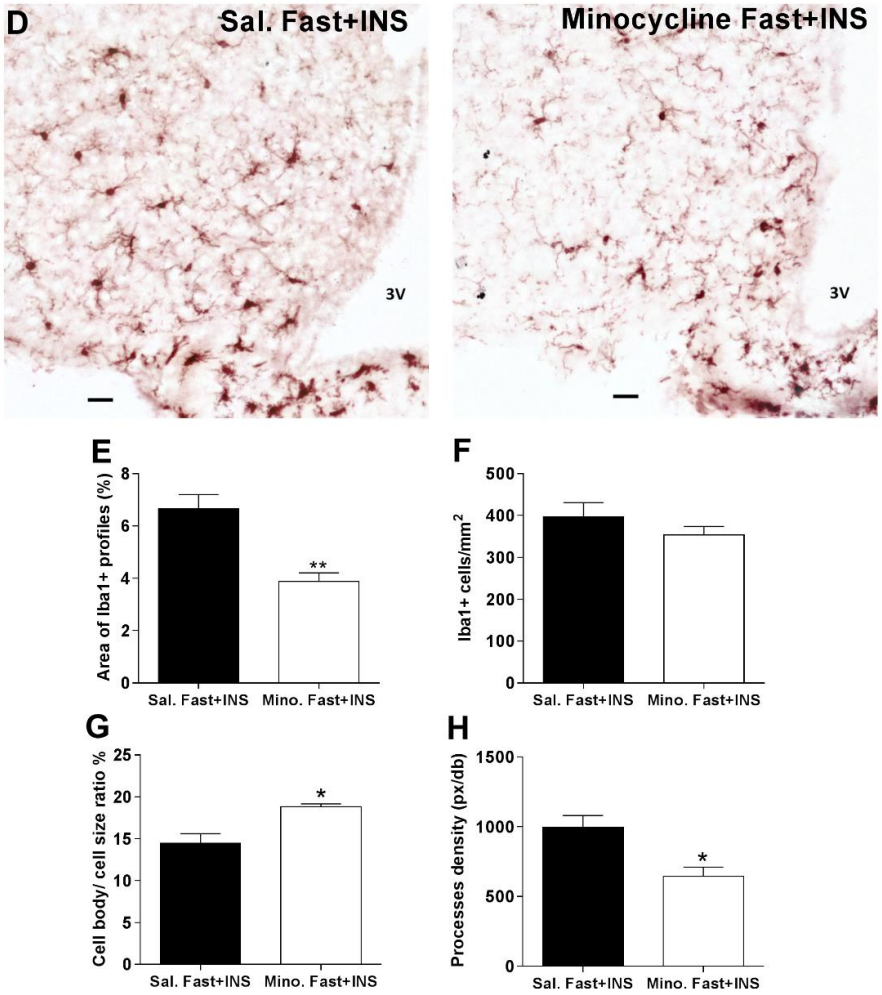

Fig.17. Minocycline attenuates microglia activation and results in enhanced counter-regulatory response

*(A) The upper panel represents the influence of minocycline on the blood glucose level 1 h after insulin and (B) the epinephrine and (C) norepinephrine concentration from pooled plasma samples. The lower panel shows the (D) qualitative and (E,F,G,H) quantitative results of Iba1 immunostaining in the ARC. 3V is the third ventricle on the right. Scale bars represent 20 µm. Proportional area of Iba1+ profiles (E), density of Iba1+ microglial cells (F), the cell body/cell size ratio (%) (G), and the Iba1+ microglial processes density (H) in the ARC are shown. Bars represent the mean ± SEM. Data were analyzed by Student's t-test (n=4 per group). *p<0.05, **p<0.01*

DOI:10.14753/SE.2018.2148

5.5. Critical involvement of interleukin IL-1 in attenuation of counter-regulatory responses to hypoglycemia

Danger signals provoke release of proinflammatory cytokines, such as IL-1 from activated glial cells. Changes in IL-1a mRNA, IL-1b mRNA expression in response to 2-deoxyglucose (2-DG) or insulin treatment were revealed using qRT-PCR analysis of cultured mouse microglia cell line (BV2) (Fig. 18A).

We found significantly elevated IL-1 mRNA level *in vivo* in hypothalamic blocks of C57BL/6 mice in response to insulin-induced hypoglycemia [Bonferroni's multiple comparisons test, $t(8)=4.925$, $p<0.01$]. By contrast, hypoglycemia-induced increase of IL-1 mRNA was not seen in mice with impaired fractalkine signaling [main effect of genotype: $F(1,8)=74.44$, $p<0.0001$] (Fig. 18B).

IL-1a/b KO mice displayed higher blood glucose concentration in response to insulin administration than wild types controls [main effect of genotype: $F(1,12)=5.02$, $p=0.045$], their blood glucose concentration did not decrease below 3 mmol/l (Fig. 18C).

Inhibition of IL-1 signaling by icv. infusion of IL-1 receptor antagonist (IL-1RA) resulted in a milder drop of blood glucose following insulin treatment compared to vehicle-injected controls, but it was not significant [$t(12)=1.658$, $p>0.05$] (Fig. 18D).

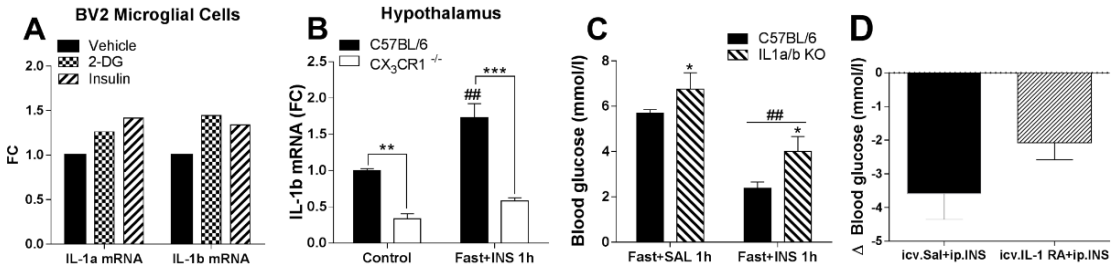

Fig.18. The role of interleukin-1 (IL-1) in attenuation of counter-regulatory responses to insulin-induced hypoglycemia

(A) IL-1a and IL-1b mRNA expression in BV2 microglial cells evoked by 2-deoxyglucose (2-DG) or insulin. (B) Hypothalamic IL-1b mRNA expression in $CX_3CR1^{-/-}$ and wild-type mice under control condition and following insulin administration. (C) Blood glucose levels of IL-1 a/b KO and wild-type mice after overnight fasting and ip. insulin administration. (D) The effect

*of icv. administered IL-1RA on the insulin-induced reduction of blood glucose concentrations in C57BL/6 mice. Bar graphs show mean values± SEM. Two-way ANOVA with Bonferroni post hoc test. The main effect of Fast+INS: ##p<0.01; $CX_3CR1^{-/-}$ vs. C57BL/6: *p<0.05, **p<0.01, ***p<0.001.*

5.6. Effects of high-fat diet (HFD) as a chronic metabolic stress model on $CX_3CR1^{-/-}$ mice

5.6.1. HFD induced-obesity

11 weeks of high-fat diet resulted in significant body weight gain in mice [main effect of HFD: $F(1,8)=16.32$, $p=0.004$], but the body weights of $CX_3CR1^{-/-}$ mice were significantly lower than HFD fed C57BL/6 mice [Bonferroni's multiple comparisons test, $t(8)=4.435$, $p<0.01$] (Fig.19A).

5.6.2. Fractalkine receptor deficiency restrained microglial activation in chronic HFD-fed mice in the ARC

Immunostaining for the microglial marker Iba1 revealed significant microglial activation in the arcuate nucleus of the hypothalamus (Fig. 19B) of HFD-fed wild-type mice [Bonferroni's multiple comparisons test, $t(7)=3.5$, $p<0.05$]. However, the area of Iba1+ cells in the ARC was significantly smaller in the fractalkine receptor deficient mice fed a HFD compared to C57BL/6 mice [Bonferroni's multiple comparisons test, $t(7)=3.5$, $p<0.05$] (Fig. 19C).

DOI:10.14753/SE.2018.2148

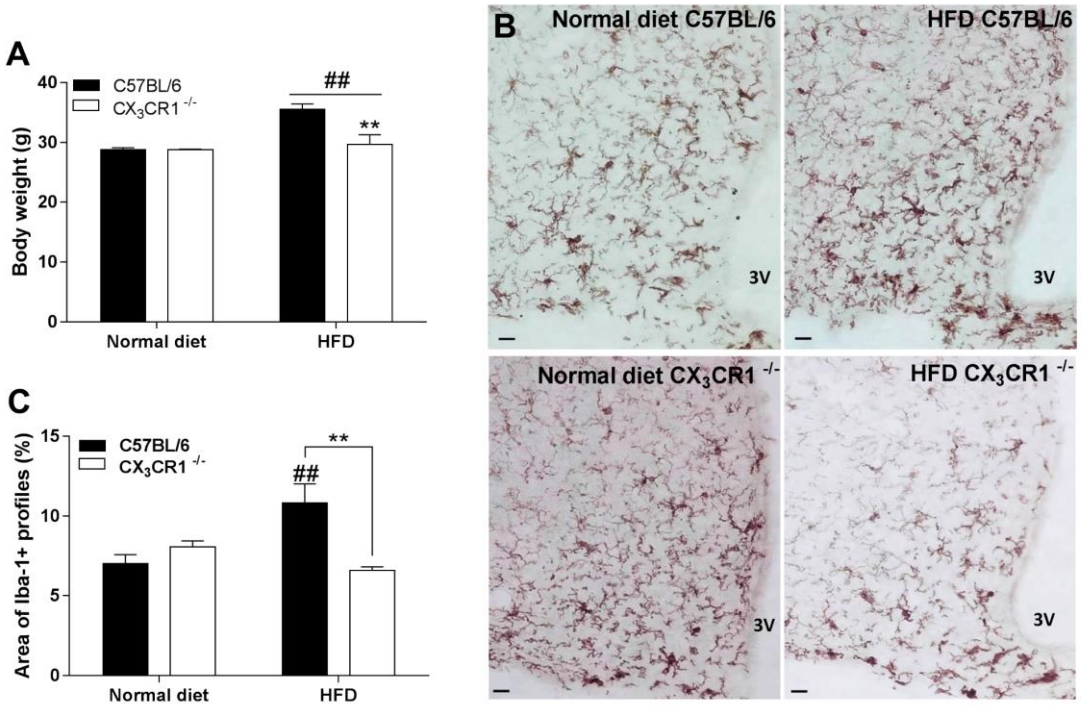

Fig.19. High-fat diet (HFD) induced body weight gain and microgliosis in the arcuate nucleus of the hypothalamus

*(A) Body weight of C57BL/6 and $CX_3CR1^{-/-}$ mice on normal diet or 11 weeks of HFD. (B) Representative photomicrographs of Iba1 immunohistochemistry within the arcuate nucleus of the hypothalamus (ARC). 3V is the third ventricle on the right. Scale bars indicate 20 µm. (C) The percentage (%) of the area occupied by Iba1+ profiles in normal diet, and HFD fed C57BL/6 and $CX_3CR1^{-/-}$ mice in the ARC (between bregma -1.22 and -1.94). Bar graphs represent mean values± SEM. Two-way ANOVA with Bonferroni post hoc test. The main effect of HFD: ##p<0.01; $CX_3CR1^{-/-}$ vs. C57BL/6: **p<0.01.*

5.6.3. Fractalkine receptor deficient mice increase thermogenesis and display cold tolerance to acute cold stress

Core body temperature of mice from both genotypes was similar at the start of cold tolerance test (35.0-35.8 °C). There was a significant drop in the core temperature in both genotypes at 60 min and 120 min cold time points (Fig. 20A). High fat fed mice showed better cold tolerance than mice on normal diet. Furthermore, after 120 min in cold, the core temperature of normal diet- and HFD fed $CX_3CR1^{-/-}$ mice reached the minimum, and started to increase back to the normal (Fig. 20B). In contrast, the core

DOI:10.14753/SE.2018.2148

temperature of heterozygous $CX_3CR1^{+/-}$ mice decreased after 120 min in cold [main effect of genotype: $F(1,26)=4.75$, $p<0.05$].

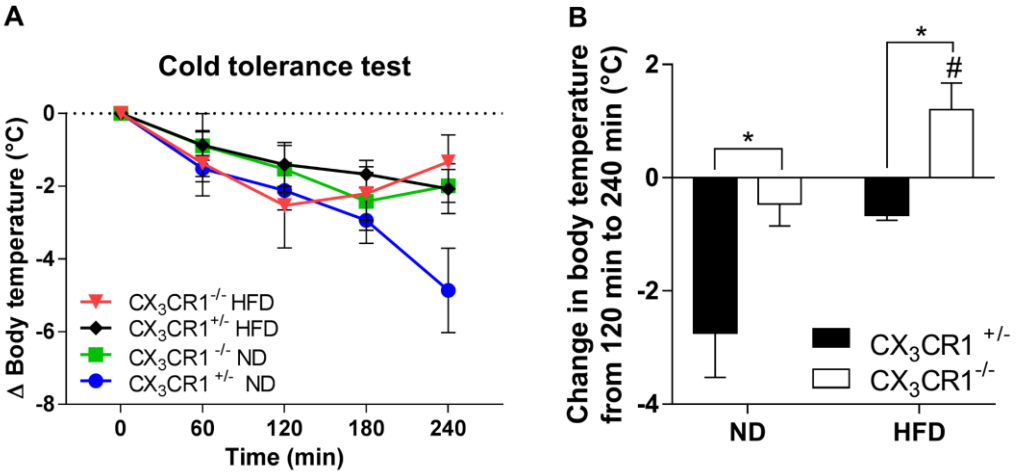

Fig.20. $CX_3CR1^{-/-}$ mice displayed improved thermogenesis to cold exposure

*(A) Time course of changes in core body temperature during cold stress. (B) Changes in body temperature between 120 min and 240 min in cold. Graphs show mean values± SEM. Two-way ANOVA with Bonferroni post hoc test. The effect of HFD: #p<0.05; $CX_3CR1^{-/-}$ vs. C57BL/6: *p<0.05. Abbreviations: ND, normal diet; HFD, high-fat diet [80]*

DOI:10.14753/SE.2018.2148

6. Discussion

6.1. Behavioral alterations in $CX_3CR1^{-/-}$ mice

Fractalkine receptor deficiency did not influence the locomotor activity of mice in their own home cage and in a novel environment (open field) neither in the active, nor in the inactive phase of the daily cycle under basal conditions and during overnight fasting. However, significantly increased locomotor activity of $CX_3CR1^{-/-}$ mice was detected in the home cage during insulin-induced hypoglycemia, which is considered as a severe metabolic stress.

Our results indicate a trend towards attenuated anxiety-like behavior in $CX_3CR1^{-/-}$ mice. These data were recently confirmed by [81] using two different anxiety tests, the light-dark box and elevated zero maze.

$CX_3CR1^{-/-}$ mice display active coping behavior in tests with significant stress component, in forced swim-, and tail suspension tests and display improved physiological compensatory mechanisms during hypoglycemia and cold stress.

Stress coping strategy is under complex regulation in which neuroendocrine, autonomic, metabolic and immune mechanisms have been implicated [82]. Increased mobilization of energy stores and energy expenditure seen in fractalkine receptor deficient animals under basal condition and after CVS may contribute to their active stress coping. Important physiological role of stress hormones, CORT and adrenaline is to mobilize glucose and free fatty acids (FFAs) to support increasing energy demands during stress.

Although we did not detect significant effects of genotype on anxiety-related behavior of chronically stressed animals in EPM and open field test, but CX_3CR1 deficient mice were resilient to chronic stress-induced anhedonia, one of major symptom of chronic stress-induced depressive like behavior. Our data are in agreement with several recent reports using different chronic challenge paradigms [66]. For instance, Hellwig et al. in a chronic despair model found that fractalkine receptor deficient mice maintain active struggling during repeated forced swim and this is related to lack of microglial morphological activation in the dentate gyrus [83]. To further support the role of neuron-microglia communication through the fractalkine pathway to drive depressive behavior, Milior et al. observed, that $CX_3CR1^{-/-}$ mice did not display liking-type anhedonia using a home cage unpredictable mild stress paradigm [84]. Resistance of

fractalkine receptor deficient mice to chronic stress-induced depression is in sharp contrast with the prolonged sickness behavior of these animals when exposed to LPS [67], highlighting major differences in the pathomechanism of depressive and sickness behavior induced by psychogenic stressors or by immune challenges, respectively.

6.2. Stress-induced activation of HPA axis and extended brain stress system - differences in $CX_3CR1^{-/-}$ mice

Acute forced swim and restraint as psychogenic stressors and hypoglycemia as a physiological/metabolic stressor stimulate the hypothalamo–pituitary–adrenocortical (HPA) axis as demonstrated by increased plasma ACTH and corticosterone levels in C57BL/6 mice. These, well-established secretory changes run in parallel with the activation of corticotropin-releasing hormone (CRH) containing parvocellular neurosecretory neurons in the hypothalamic paraventricular nucleus as revealed by appearance of c-Fos immunoreactive (-ir) cell nuclei. *c-fos* is an immediate early gene (IEG), which is transiently induced by different acute cellular challenges and is a valuable tool to identify activated neurons throughout the brain [85]. Using this IEG based functional mapping strategy, we have confirmed acute stress-induced neuronal activation in the hypothalamic paraventricular nucleus (PVN) in response to physiological (metabolic) and psychogenic challenges. However, the time course of c-Fos induction in the PVN is stressor dependent. Previous studies from our laboratory have shown that IEG expression in the PVN peaks 30 min after restraint but at 60 min after hypoglycemia and returns to baseline by 240 min after challenge in both cases [79].

In addition to the final arm of the neuroendocrine axis, stressful events activate a variety of brain regions and extended circuitries, which convey stress-related information to the neurosecretory neurons. In our condition, single ip. insulin (1 IU/kg) administration following overnight fasting resulted in significant drop of blood glucose concentration (below 3 mmol/l) in mice, which was accompanied with the elevation of plasma corticosterone level and enhanced c-Fos immunoreactivity in number of stress-related and glucose- sensitive brain regions, including cerebral cortex, lateral septum, bed nucleus of stria terminalis, thalamic paraventricular nucleus, amygdala, various hypothalamic (lateral-, paraventricular-, periventricular-, ventromedial-, dorsomedial-

and arcuate) and brainstem nuclei (lateral parabrachial nucleus and nucleus of the solitary tract). There are stressor-specific regions, which became activated in challenge specific manner [7]. For instance, insulin-induced hypoglycemia dramatically activates neurons in the arcuate region, however psychogenic stressor evoke only a weak –to-moderate c-Fos staining in this nucleus, confirming stressor-specific recruitment of hypothalamic neurons. Furthermore, both humoral and neuronal pathways are necessary for the activation of HPA axis, and the severity of insulin-induced hypoglycemia determines which pathways are triggered [86].

Increased c-Fos expression co-localized with CRH-producing neurons in the hypothalamus and with tyrosine hydroxylase (TH) in the A2 area of brainstem rats exposed to acute 3 IU/kg insulin dose [7]. In my experiments, co-localization of NPY or POMC mRNA with c-Fos protein in the medial basal hypothalamus revealed selective activation of orexigenic NPY neurons triggered by insulin-induced hypoglycemia. Furthermore, relative expression of NPY and AgRP mRNAs have been elevated two fold in the arcuate nucleus, while POMC expression was unchanged.

In addition to the neuroendocrine stress axis, internal and external challenges activate sympathyo-adrenal and sympatho-neuronal systems [7] resulting in elevation of plasma adrenaline and extracellular noradrenaline concentrations, respectively.

Because of the transient nature of IEG induction, repeated or chronic challenges do not result in persistent *c-fos* expression, therefore we did not detected c-Fos-ir in the brain of animals that have been exposed to maternal separation and/or chronic variable stress paradigm. However, this does not necessarily mean the lack of chronic load on these pathways. It has been shown that repeated restraint stress caused the habituation of c-fos response [87], but chronic/repeated hypoglycemia provoked marked increases in c-Fos and CRH mRNA in the PVN [88]. Additional variable in stress reactivity is the strain of the animals. Stress-sensitive, BALB/c mice show different brain activation patterns to acute restraint compared to C57BL/6 mice. In this case, cingulate cortex hypoactivation was associated with highly anxious phenotype of BALB/c mice [89].

Next, we have been interested whether the neuroendocrine stress reaction is different in $CX_3CR1^{-/-}$ mice in which one aspect of the neuron-to-microglia communication is

absent. Real-time quantitative PCR measurement revealed that basal CRH mRNA expression in the hypothalamus was significantly higher in $CX_3CR1^{-/-}$ mice than wild-type mice. The hypothalamo-pituitary-adrenocortical axis is more responsive to acute psychological stressors (FST, restraint) in $CX_3CR1^{-/-}$ animals, compared to wild-type C57BL/6 controls, as revealed by increased c-Fos activation in the PVN and elevated stress-induced plasma hormone levels (ACTH, CORT). However, we did not detect any difference between the genotypes in HPA-axis reactivity after acute insulin-induced hypoglycemia. Hypoglycemia, as a systemic stressor activate direct projections to the CRH neurons in the PVN from catecholaminergic neurons in the brainstem, but restraint as a psychogenic stressor signal through multisynaptic pathway [90]. Therefore, increased restraint stress-induced neuronal activation in the PVN of $CX_3CR1^{-/-}$ mice might be related to impaired inhibitory control originating in the prefrontal cortex and hippocampus [91]. To support this hypothesis, it has been shown that $CX_3CR1^{-/-}$ mice have developmental impairments with delayed excitatory synaptic pruning in the hippocampus [92] resulting immature connectivity in the knockout animals.

We also found exaggerated hypothalamic CRH mRNA response of fasted $CX_3CR1^{-/-}$ animals following insulin injection compared to C57BL/6 controls. Furthermore, fractalkine receptor deficient mice showed significantly higher hypothalamic NPY and AgRP mRNA transcription to insulin-induced hypoglycemia than wild-type animals.

By contrast, we did not detect overt genotype effect in chronic psychogenic stress-induced differences in CRH expression, plasma corticosterone levels and adrenal weights. Relative thymus weights were lower in MS+CVS exposed, $CX_3CR1^{-/-}$ animals indicating elevated corticosterone load during intervention.

Exposure of high fat diet represents a chronic metabolic stress as revealed by elevated ACTH and CORT levels in obese animals [93]. Our group has confirmed this finding [94], however, similar to the situation seen in chronic psychogenic stress, we did not detect any significant effect of genotype on hormonal variables.

DOI:10.14753/SE.2018.2148

6.3. CX_3CR1 dependent, stress-induced activation of hypothalamic microglia

In addition to activation of brain stress circuits, it has been recently shown that stressor exposure evoke local and systemic sterile inflammatory response [95], which is associated with stress-induced danger-associated molecular patterns, DAMPS or alarmins [96-99]. Because microglia respond to PAMPs and DAMPs and increase inflammatory proteins, it might be hypothesized that microglia may be activated by systemic and/or cellular stressors. Indeed, in response to metabolic stressors, hypoglycemia and high fat diet, we revealed signs of microglia activation in the hypothalamus. In the case of hypoglycemia, the number and the density of Iba1+ profiles was increased, while the nearest neighbor distance and the spacing index decreased, suggesting recruitment of microglia as early as 1h after insulin injection, at the nadir of blood glucose concentration. Interestingly, activated microglia was seen in the close proximity of c-Fos positive, activated neurons in the arcuate nucleus. Furthermore, confocal analysis of this region confirmed that microglia make contacts with the activated neurons. Recruitment of microglia seems to be region specific, since microglia was activated in the arcuate- but not in the paraventricular nucleus of hypoglycemic mice. Such a heterogenous microglia response is seen in animals exposed to acute psychogenic stressors. For instance, inescapable tail shock [100] and repeated restraint [101] activated microglia in the hippocampus ad prefrontal cortex respectively. However, we failed to detect any significant psychogenic stress-induced changes in the hypothalamic microglia. These results are in contrast with those published by Sugama et al. reporting microglia activation throughout many brain regions including hypothalamus, thalamus, hippocampus, substantia nigra and central gray following restraint stress combined with water immersion [102]. One possible explanation for this difference would be the intensity of the stressors, restraint alone is a much milder stressor than restraint combined with water immersion.

It has been shown that chronic stress induces differential microglia activation along the brain stress axis: mPFC, hippocampus, nucleus accumbens, amygdala, dBNST and lPAG display significant activation following repeated restraint [103], while the density and morphology of hypothalamic (PVN) microglia is not altered in response to chronic

homotypic or heterotypic stress regimens [104]. Our findings support these data. Using a different, non-habituating chronic stress procedure (two hits stress paradigm, a combination of early life adversity with chronic unpredictable stress challenge in the adulthood) our present results suggest that either chronic stressors do not engage PVN microglia or that HPA activation is sufficient to keep microglia activation under control [105].

Factors initiating stress-induced microglia activation remain largely unknown. Putative DAMPs include extracellular heat-shock protein 72 (Hsp72), uric acid crystals, high-mobility group box 1 (HMGB1), and adenosine triphosphate (ATP) [97]. There is a significant overlap between cytokines and chemokines induced by pathogen activated molecular patterns (PAMPS, ie LPS) and DAMPS. Furthermore, it has been also shown that some features of the sterile inflammatory response after stressor exposure are dependent on NLRP3 inflammasome [98].

Binding of fractalkine to fractalkine receptor has been suggested as being an "off" signal to microglia [48], therefore, absence of the receptor in CX3CR1-/- animals have been thought to result in activation even under basal, no-stress conditions. Light microscopic analysis, however, does not detect overt morphological signs of microglia activation in the hypothalamus under resting, control state. These results confirm previous findings on the density of Iba1 positive profiles in the dentate gyrus of unstressed wild-type and $CX_3CR1^{-/-}$ mice [83] but are in contrast to those found by Milior et al. [84] in the CA1 stratum radiatum.

In response to acute psychogenic or physiological stressors, microglia activation was somehow attenuated in $CX_3CR1^{-/-}$ mice compared to the wild type. Morphological parameters of microglia, including the number, the density and the nearest neighbor distance decrease after acute stress suggesting non-responsivity of hypothalamic microglia to stressful challenges. It should be noted, however, that we did not find genotype-specific changes of glia morphology in chronically stressed animals. Along these lines, Hellwig et al. in a chronic despair model revealed that fractalkine receptor deficient mice do not exhibit stress-induced changes in microglia morphology in the dentate molecular layer [83] and Milior et al. observed attenuated stress-induced

changes in CA1 microglia (morphology, phagocytosis) and neuronal (reduction in long term potentiation) properties in $CX_3CR1^{-/-}$ mice using a home cage unpredictable mild stress paradigm [84].

6.4. HFD-induced microglial activation

Diet-induced obesity is associated with a form of low-grade inflammation in peripheral tissues recruiting proinflammatory macrophages and other immune-related cells (neutrophils, mast cells, CD8+ T cells) in white adipose and other metabolic tissues [106] and is implicated in the development of insulin resistance [107]. While most studies have focused the neuronal regulation of energy balance in the CNS, relatively few have investigated the role of non-neuronal cells. During dietary excess, peripheral inflammation is accompanied by a more rapid inflammation involving glial cell accumulation (gliosis) in the hypothalamic areas critical for energy homeostasis. Increased gliosis in the mediobasal hypothalamus (MBH) of obese humans was assessed by MRI. Reactive gliosis was observed in the hypothalamic arcuate nucleus in rodents within the first week of HFD onset [108]. The function of CD36 fatty acid translocase is the uptake of monounsaturated fatty acids, which is expressed in the CNS not only by astrocytes, endothelial cells, but also by microglial cells [109], thus resident microglia can detect fatty acids directly. The first mechanistic evidence that microglia orchestrate both the immunologic and physiologic responses of the hypothalamus to dietary excess was provided by Valdearcos et al [110]. They showed that selectively depletion microglia with CSF1R phosphatase inhibitor PLX5622 and genetically restraining the inflammatory responsiveness of microglia through NF-κB-mediated inflammatory signaling protected HFD-fed mice from hyperphagia and diet-induced obesity. By contrast, activating resident microglia was sufficient to recruit bone-marrow-derived myeloid cells into the MBH and to elicit diet-independent weight gain which was associated with increased food intake, reduced whole-body energy expenditure and reduced leptin sensitivity.

Because fractalkine/fractalkine receptor (CX_3CR1) pathway plays a key role in recruitment, infiltration and proinflammatory polarization of macrophages and microglial cells, we compared the HFD-induced changes in the hypothalamic microglia in $CX_3CR1^{-/-}$ and wild-type mice. My results demonstrate that fractalkine receptor

deficiency restrained microglial activation in the arcuate nucleus in chronic HFD-fed mice. Other reports from the literature support this notion, for instance, inhibition of hypothalamic fractalkine with siRNA in HFD fed, obesity-prone Swiss mice resulted in reduction of hypothalamic inflammation via the decreased recruitment of the bone-marrow derived cells into the hypothalamus, which was accompanied by the reduction of obesity and improvement of glucose intolerance. It has been proposed that the rapid resident microglial activation in response to dietary fats induce expression of fractalkine by hypothalamic neurons, and fractalkine is the key activator of hypothalamic inflammation by controlling the recruitment of pro- and anti-inflammatory macrophages to the hypothalamus [111]. Intriguingly, CX_3CR1 deficiency affected whole body metabolism beyond hypothalamic microglia. $CX_3CR1^{-/-}$ mice gain significantly less weight and adipose tissue of fat-enriched diet than heterozygote controls. The fractalkine receptor deficient mice kept on HFD do not develop glucose intolerance and display less adipose inflammation [94]. Furthermore, fractalkine receptor deficiency selectively attenuated the expression of certain proinflammatory cytokines (TNF-α, IL-1α, Ccl2) in the brown adipose tissue (BAT), and increased the expression of lipolytic enzymes in BAT [80].

6.5. Microglial activation evoked by insulin induced hypoglycemia

Glucose is the main energy source of the CNS, but ketone bodies (lactate, pyruvate, ketones) also can be used by neurons as an alternative energy source and function as metabolic signals. Changes in glucose concentration are quickly detected by glucose-sensing neurons in hypothalamus and glial cells might also be involved in the glucose-sensing mechanisms. Astrocytes are able to synthesize lactate or glucose from glycogenolysis during fasting. If glycogen stores are exhausted, astroglial cells can produce ketone bodies by utilization of fatty acids, and provide these as alternative energy source for neurons and acting as energy availability signals [109]. Microglia are also able to sense metabolic, hormonal and injury- or infection-related signals via their, receptors, transporters and ion channels. Among others, microglia express glucose transporter 5 (GLUT5), monocarboxylate transporters (MCT1, MCT2), pattern-recognition receptors (TLRs) and numerous other receptors for neurotransmitters, neurohormones, cytokines, chemokines [112]. Microglial cells are equipped with

K(ATP) channel components SUR-1 or SUR-2, together with glucokinase and sensitive to extracellular glucose concentration [113]. It has recently been shown that fasting, via ghrelin rise and low glucose, suppresses Na^+/K^+ - ATPase enzyme/pump activity in ARC and thereby promotes the activation of GI neurons and NPY/AgRP-dependent feeding [114]. The activational role of extracellular ATP during hypoglycemia can also be hypothesized. Extracellular ATP is a strong microglia activator signaling through P2X7 receptors [115]. For instance, during oxygen glucose deprivation (OGD) (i.e. ischemic stroke) ATP levels increase dramatically and activates microglia via purin receptors (P2X7) and results in release of proinflammatory cytokine, IL-1b [116].

Hypoglycemia resulted in selective microglial activation within the hypothalamic arcuate nucleus of C57BL/6 mice compared to fed and fasted controls, as revealed by morphometrical analysis of ionized calcium-binding adaptor molecule 1 (Iba1) immunostained sections. This microglial rearrangement was specific for the medial basal hypothalamus/arcuate nucleus/median eminence region and not seen in other hypothalamic (i.e. PVN) or limbic (hippocampus) structures, suggesting that the signal for microglial cells may originate specifically in this region.

In the arcuate nucleus of hypoglycemic animals, microglia displayed activated phenotype with thickened branches, enhanced Iba1-immunoreactivity, and increased the density of Iba1 positive cells. Furthermore, these "thickened" microglial cells were recruited around orexigenic NPY^+/ $c\text{-}Fos^+$, activated neuron population in the rostral and medial portion of the arcuate nucleus, and close appositions were detected between microglial processes and activated neurons in the ARC. This morphological scenario shows some similarities to those seen in the cerebral cortex after traumatic, ischemic or cellular injuries as imaged by two photon microscopy [34].

Fractalkine receptor (CX_3CR1) is critically implicated in activation of microglia to physiological and traumatic insults. Indeed, microglia with "resting" or "non-responding" phenotype were found in $CX_3CR1^{-/-}$ mice around NPY^+/ $c\text{-}Fos^+$ neurons following insulin challenge. Moreover, we revealed exaggerated hypothalamic NPY and AgRP mRNA expression in the fractalkine receptor deficient mice to insulin-induced hypoglycemia compared to wild-type animals.

To directly challenge the role of microglia in insulin-hypoglycemia, we have used minocycline, a tetracyclin antibiotic which is frequently used for inhibition of microglia

in vivo and in vitro [117]. Minocycline treated mice displayed less severe hypoglycemia following insulin treatment, suggesting that impaired microglia function may result in improved glucose counter-regulatory responses.

6.6. The role of microglial IL-1 in compromised compensatory responses to hypoglycemic stress

Danger signals provoke release of proinflammatory mediators, such as IL-1, IL-6 and TNFa from activated microglia. Interleukin-1b (IL-1b) is a pleiotropic proinflammatory cytokine [118], which regulates peripheral and central immune processes, but it can also contribute to physiologic functions, such as activation of the HPA axis, and -in the periphery, modulation of insulin secretion by pancreatic islets [119], or in the brain such as maintaining of long-term potentiation in hippocampus [120]. The expression of IL-1b is evoked in the brain during increased neuronal activity and acute stress conditions [121]. The brain-borne IL-1b affects thermoregulation, neuroendocrine stress responses through noradrenergic, serotonergic, glutamatergic and CRH-producing neuronal pathways [122, 123]. Furthermore, intracerebroventricular administration of IL-1b caused long-lasting and profound hypoglycemia in absence of adequate neuroendocrine and behavioral counter regulation. Furthermore, despite of hypoglycemia, IL-1b stimulates brain metabolism, facilitates glucose uptake by neurons and astrocytes [123].

We detected increased pro-inflammatory IL-1a and IL-1b mRNA expression *in vitro* in BV2 microglia treated with insulin or 2-DG, implicating that microglia (at least in culture) are directly sensitive to insulin and glucopenia and able to synthesize IL-1a and IL-1b in response to these challenges. Although it has been shown in human cell culture system, that microglia express both isoforms of the insulin receptor, and insulin receptor substrates (IRS-1, IRS-2), which are required for propagation of insulin/IGF-1 signaling, it has been hypothesized that additional factors, such as extracellular ATP and fractalkine, released from glucose sensitive neurons or astrocytes might play a role in activation of microglia in vivo acting on microglial P2X7 and CX_3CR1 receptors, respectively [124].

Indeed, we have revealed increased IL-1a and IL-1b mRNA levels in the hypothalamic blocks of mice exposed to insulin following overnight fasting. By contrast, attenuated

hypothalamic expression of insulin hypoglycemia-induced IL-1 in $CX_3CR1^{-/-}$ mice, do implicate the involvement of fractalkine signaling in glucopenia. Furthermore, improved glucose compensation is seen in animals with defective fractalkine receptor and attenuated IL-1 expression. In addition, $CX_3CR1^{-/-}$ mice mount increased NPY/AgRP and sympatho-adrenal responses to hypoglycemia.

To address the role of IL-1 in the full development of counter-regulatory mechanisms to glucopenia, we tested the effects of IL-1RA in wild type, C57BL/6 mice. IL-1RA is a naturally occurring peptide antagonist, which inhibits proinflammatory activity of both IL-1a and IL-b. Central administration of recombinant IL-1RA prior to insulin injection, resulted in a much less severe drop of blood glucose following hypoglycemic challenge, compared to vehicle injected group.

Finally, we injected insulin to fasted IL-1a/b KO mice and found that these animals were resistant to hypoglycemic action of insulin, i.e. they mount improved counter-regulatory mechanisms.

The bacterial lipopolysaccharide, LPS also results in hypoglycemia, which is dependent of IL-1 [125, 126]. Furthermore, central, rather than peripheral IL-1 is responsible for these changes [123]. Our present result suggest that insulin-induced hypoglycemia is also dependent on central microglial IL-1 a/b signaling.

These findings might have clinical significance. Hypoglycemia associated autonomic failure (HAAF) is a serious condition, which is relatively often develops in diabetic patients under intense insulin treatment [127]. The key feature of HAAF is the defective counter-regulation. Our present results highlight that ongoing infections, inflammation (neuroinflammation), which are accompanied by elevated IL-1 levels might interfere with the full development of hypoglycemia-induced physiological responses.

DOI:10.14753/SE.2018.2148

7. Conclusions

The main conclusions of my dissertation are:

1. **Acute and chronic-, physiological, metabolic and psychogenic stressors activate hypothalamic microglia in stress- and site-specific manner.**

   I have provided new evidence for that:

   - acute insulin induced-hypoglycemia and chronic exposure to high-fat diet (HFD) trigger robust microglial activation in the hypothalamic arcuate nucleus.
   - acute and chronic psychogenic stressors results only weak microglial activation in the hypothalamic paraventricular nucleus.

2. **The fractalkine-fraktalkine receptor signaling between neurons and microglia contributes to stress-induced activation of microglia.**

   I have shown that the absence of functioning CX_3CR1 in $CX_3CR1^{-/-}$ mice

   - attenuates activation of microglial cells in the arcuate nucleus of the hypothalamus induced by acute hypoglycemia and chronic high-fat diet exposure.

3. **Impaired fractalkine signaling supports active coping with improved activational- hormonal- and counter-regulatory responses.**

   I have found that mice with non-functioning fractalkine receptor ($CX_3CR1^{-/-}$) represent:

   - heightened energy expenditure and increased hypothalamic CRH expression
   - exaggerated neuronal activation in the hypothalamic paraventricular nucleus and increased corticosterone release in response to acute restraint stress
   - active coping behavior in tests with significant stress component
   - resistance to chronic variable stress –induced anhedonia
   - display improved cold tolerance

DOI:10.14753/SE.2018.2148

I have found that the mice with targeted CX_3CR1 gene disruption

- do not develop hypoglycemia
- display enhanced locomotor activity
- release significantly higher plasma catecholamines
- overexpress NPY/AgRP counter-regulatory neuropeptides in the arcuate nucleus
- fails to upregulate hypothalamic IL-1b expression in response to overnight fasting and ip. insulin administration.

4. **Activated microglia and microglial interleukin-1 (IL-1) provide a false/ inhibitory signal to metabolic-related neurons which explain why the counter-regulatory response to hypoglycemia is not fully triggered.**

I have demonstrated that central blockade of microglial activity by minocycline results in improved glycemic control and catecholamine response.

I have revealed that the lack of interleukin-1 in IL1a/b KO mice or central inhibition of IL-1b signaling by IL-1receptor antagonist attenuates hypoglycemic response to insulin.

DOI:10.14753/SE.2018.2148

8. Summary

Microglia, the resident immune cells of the central nervous system are sensitive to various perturbations of the environment, such as stress exposure and play a role in regulating of various homeostatic functions.

Among the pathways mediating stress-related neuronal cues to microglia, the fractalkine-fractalkine receptor (CX_3CR1) signaling has a crucial role. Fractalkine is a key regulator of microglial activity and involved in neuron-microglia communication upon binding to its' specific receptor, CX_3CR1 on microglial cells.

In my dissertation I aimed to reveal the role of hypothalamic microglia via fractalkine signaling in modulation of stress response induced by acute or chronic exposure of psychogenic or physiological stressors. By using mice, in which the fractalkine receptor gene was disrupted ($CX_3CR1^{-/-}$), we explored hormonal and behavioral responses to acute and chronic stressful stimuli along with changes in hypothalamic microglia.

I demonstrated that $CX_3CR1^{-/-}$ mice display active coping behavior in tests with significant stress component, have enhanced HPA response to acute psychogenic stress and resistance to chronic variable stress–induced anhedonia, which is accompanied by the reduction of microglia in the hypothalamic paraventricular nucleus. Acute severe hypoglycemia and chronic exposure to high-fat diet (HFD) stimulate robust microglial activation in the hypothalamic arcuate nucleus. However, the microglial alterations induced by metabolic challenges are attenuated in fractalkine receptor deficient mice. Furthermore, I found that impaired neuron-microglia communication in mice, results in improved glycemic control in response to insulin-induced hypoglycemia due to increased transcriptional and hormonal counter-regulatory responses. In addition, I have revealed that microglial IL-1 provide a false/ inhibitory signal to metabolic-related neurons and explain why the counter-regulatory response to hypoglycemia is not fully triggered.

These results highlight differential involvement of microglia and fractalkine signaling in controlling/integrating hormonal-, metabolic and behavioral responses to acute and chronic stress challenges.

DOI:10.14753/SE.2018.2148

9. Összefoglalás

A mikroglia, a központi idegrendszer immunsejtjeként képes detektálni számos külső, szervezetet veszélyeztető hatást, mint pl. a stressz és részt vesz a homeosztatikus folyamatok helyreállításában.

A stressz által aktivált neuronok és a mikroglia sejtek közti kommunikációban jelentős szerepet játszik a fraktalkin-fraktalkin receptor (CX_3CR1) szignalizáció. Az idegsejtek által termelt fraktalkin specifikus receptora a mikroglia sejteken fejeződik ki, ezáltal a mikrogliális aktivitás egyik fő szabályozó molekulája.

A disszertációmban célul tűztem ki, hogy feltárjam a fraktalkin jelátviteli útvonalon keresztül hipotalamikus mikroglia sejtek szerepét az akut és krónikus-, pszichogén illetve metabolikus stresszorok által indukált stresszválaszban. Ennek érdekében az akut és krónikus stresszorokra adott hormonális, viselkedésbeli válaszokat, valamint a hipotalamikus mikroglia sejtek változásait genetikailag módosított, fraktalkin receptor deficiens egereken ($CX_3CR1^{-/-}$) vizsgáltam.

Kísérleteimmel igazoltam, hogy $CX_3CR1^{-/-}$ egerek inkább választják az aktív megküzdési stratégiát jelentős stressz komponenst tartalmazó tesztekben, fokozott HPA-tengely aktiválódást mutatnak akut pszichogén stresszre, viszont rezisztensek a krónikus variábilis stressz által indukált anhedónia kialakulására. Ezen változásokkal párhuzamosan mikroglia sejtszám csökken a hipotalamusz paraventrikuláris magjában. Akut hipoglikémia, illetve hosszú ideig tartó magas zsírtartalmú diéta markáns mikroglia aktivációt idéz elő a hipotalamusz arcuatus magjában. Fraktalkin receptor hiányában jelentősen kisebb mértékű hipotalamikus mikroglia aktiváció alakul ki a metabolikus kihívások hatására. Továbbá, a működőképes fraktalkin receptor hiánya fokozott transzkripciós és hormonális ellenregulációs választ tesz lehetővé inzulin-indukálta hipoglikémiára. Bemutattam, hogy a mikroglia eredetű IL-1 citokin téves/gátló jelként szolgálhat a metabolizmust szabályozó neuronok felé és ezáltal a glukóz csökkenésre adott ellenregulációs folyamatok jelentősen gyengülnek. .

Ezek az eredmények hozzájárulnak az akut és a krónikus stresszorokra adott hormonális, metabolikus és viselkedésbeli válaszok, a mikroglia sejtek és a fraktalkin szignalizáció által szabályozott folyamatok összefüggéseinek megismeréséhez.

DOI:10.14753/SE.2018.2148

10. Bibliography

1 Cannon W. (1929) Organization for physiological homeostasis. Physiol Rev, (9): 399–431.

2 Selye H. (1936) A syndrome produced by diverse nocious agents. Nature (138): 32.

3 Selye H. (1950) The physiology and pathology of exposure to stress. A treatise based on the concepts of the general adaptation syndrome and the diseases of adaptation. Montreal: Acta Inc.

4 Sterling P EJ. Allostasis: a new paradigm to explain arousal pathology. In: Fisher S, Reason J (eds.), Handbook of life stress, cognition and health. NY: John Wiley & Sons, New York, 1988: 629-649.

5 de Kloet ER, Joels M,Holsboer F. (2005) Stress and the brain: from adaptation to disease. Nat Rev Neurosci, 6(6): 463-75.

6 McEwen BS. (1998) Protective and damaging effects of stress mediators. N Engl J Med, 338(3): 171-9.

7 Pacak K,Palkovits M. (2001) Stressor specificity of central neuroendocrine responses: implications for stress-related disorders. Endocr Rev, 22(4): 502-48.

8 Herman JP, Figueiredo H, Mueller NK, Ulrich-Lai Y, Ostrander MM, Choi DC,Cullinan WE. (2003) Central mechanisms of stress integration: hierarchical circuitry controlling hypothalamo-pituitary-adrenocortical responsiveness. Front Neuroendocrinol, 24(3): 151-80.

9 Sawchenko PE, Brown ER, Chan RK, Ericsson A, Li HY, Roland BL,Kovacs KJ. (1996) The paraventricular nucleus of the hypothalamus and the functional neuroanatomy of visceromotor responses to stress. Prog Brain Res, 107: 201-22.

10 Sawchenko PE,Swanson LW. (1982) The organization of noradrenergic pathways from the brainstem to the paraventricular and supraoptic nuclei in the rat. Brain Res, 257(3): 275-325.

11 Swanson LW,Sawchenko PE. (1983) Hypothalamic integration: organization of the paraventricular and supraoptic nuclei. Annu Rev Neurosci, 6: 269-324.

12 Kovacs KJ,Sawchenko PE. (1996) Sequence of stress-induced alterations in indices of synaptic and transcriptional activation in parvocellular neurosecretory neurons. J Neurosci, 16(1): 262-73.

13 Herman JP, Tasker JG, Ziegler DR,Cullinan WE. (2002) Local circuit regulation of paraventricular nucleus stress integration: glutamate-GABA connections. Pharmacol Biochem Behav, 71(3): 457-68.

14 Herman JP. (2017) Regulation of Hypothalamo-Pituitary-Adrenocortical Responses to Stressors by the Nucleus of the Solitary Tract/Dorsal Vagal Complex. Cell Mol Neurobiol, 38(1): 25-35.

15 Ghosal S, Packard AEB, Mahbod P, McKlveen JM, Seeley RJ, Myers B, Ulrich-Lai Y, Smith EP, D'Alessio DA,Herman JP. (2017) Disruption of Glucagon-Like Peptide 1 Signaling in Sim1 Neurons Reduces Physiological and Behavioral Reactivity to Acute and Chronic Stress. J Neurosci, 37(1): 184-193.

16 Maruyama M, Matsumoto H, Fujiwara K, Noguchi J, Kitada C, Fujino M,Inoue K. (2001) Prolactin-releasing peptide as a novel stress mediator in the central nervous system. Endocrinology, 142(5): 2032-8.

17 Konczol K, Bodnar I, Zelena D, Pinter O, Papp RS, Palkovits M, Nagy GM,Toth ZE. (2010) Nesfatin-1/NUCB2 may participate in the activation of the hypothalamic-pituitary-adrenal axis in rats. Neurochem Int, 57(3): 189-97.

18 Maniscalco JW, Zheng H, Gordon PJ,Rinaman L. (2015) Negative Energy Balance Blocks Neural and Behavioral Responses to Acute Stress by "Silencing" Central Glucagon-Like Peptide 1 Signaling in Rats. J Neurosci, 35(30): 10701-14.

19 Sawchenko PE,Swanson LW. (1983) The organization and biochemical specificity of afferent projections to the paraventricular and supraoptic nuclei. Prog Brain Res, 60: 19-29.

20 Katsuura G, Arimura A, Koves K,Gottschall PE. (1990) Involvement of organum vasculosum of lamina terminalis and preoptic area in interleukin 1 beta-induced ACTH release. Am J Physiol, 258(1 Pt 1): E163-71.

21 Varela L,Horvath TL. (2012) Leptin and insulin pathways in POMC and AgRP neurons that modulate energy balance and glucose homeostasis. EMBO Rep, 13(12): 1079-86.

22 Chen SR, Chen H, Zhou JJ, Pradhan G, Sun Y, Pan HL,Li DP. (2017) Ghrelin receptors mediate ghrelin-induced excitation of agouti-related protein/neuropeptide Y but not pro-opiomelanocortin neurons. J Neurochem, 142(4): 512-520.

23 Konner AC, Janoschek R, Plum L, Jordan SD, Rother E, Ma X, Xu C, Enriori P, Hampel B, Barsh GS, Kahn CR, Cowley MA, Ashcroft FM,Bruning JC. (2007) Insulin action in AgRP-expressing neurons is required for suppression of hepatic glucose production. Cell Metab, 5(6): 438-49.

24 Routh VH, Hao L, Santiago AM, Sheng Z,Zhou C. (2014) Hypothalamic glucose sensing: making ends meet. Front Syst Neurosci, 8: 236.

25 Marty N, Dallaporta M,Thorens B. (2007) Brain glucose sensing, counterregulation, and energy homeostasis. Physiology (Bethesda), 22: 241-51.

26 Parton LE, Ye CP, Coppari R, Enriori PJ, Choi B, Zhang CY, Xu C, Vianna CR, Balthasar N, Lee CE, Elmquist JK, Cowley MA,Lowell BB. (2007) Glucose sensing by POMC neurons regulates glucose homeostasis and is impaired in obesity. Nature, 449(7159): 228-32.

27 Burdakov D,Gonzalez JA. (2009) Physiological functions of glucose-inhibited neurones. Acta Physiol (Oxf), 195(1): 71-8.

28 Herman JP, McKlveen JM, Ghosal S, Kopp B, Wulsin A, Makinson R, Scheimann J,Myers B. (2016) Regulation of the Hypothalamic-Pituitary-Adrenocortical Stress Response. Compr Physiol, 6(2): 603-21.

29 Rio-Hortega PD. Microglia. In: Penfield W (eds.), Cytology and Cellular Pathology of the Nervous System. Hoeber, New York, 1932: 482–1924–534.

30 Norden DM, Muccigrosso MM,Godbout JP. (2015) Microglial priming and enhanced reactivity to secondary insult in aging, and traumatic CNS injury, and neurodegenerative disease. Neuropharmacology, 96(Pt A): 29-41.

31 Wieghofer P,Prinz M. (2016) Genetic manipulation of microglia during brain development and disease. Biochim Biophys Acta, 1862(3): 299-309.

32 Crotti A,Ransohoff RM. (2016) Microglial Physiology and Pathophysiology: Insights from Genome-wide Transcriptional Profiling. Immunity, 44(3): 505-515.

33 Ginhoux F, Lim S, Hoeffel G, Low D,Huber T. (2013) Origin and differentiation of microglia. Front Cell Neurosci, 7: 45.

34 Davalos D, Grutzendler J, Yang G, Kim JV, Zuo Y, Jung S, Littman DR, Dustin ML,Gan WB. (2005) ATP mediates rapid microglial response to local brain injury in vivo. Nat Neurosci, 8(6): 752-8.

35 Nimmerjahn A, Kirchhoff F,Helmchen F. (2005) Resting microglial cells are highly dynamic surveillants of brain parenchyma in vivo. Science, 308(5726): 1314-8.

36 Wake H, Moorhouse AJ, Jinno S, Kohsaka S,Nabekura J. (2009) Resting microglia directly monitor the functional state of synapses in vivo and determine the fate of ischemic terminals. J Neurosci, 29(13): 3974-80.

37 Hanisch UK,Kettenmann H. (2007) Microglia: active sensor and versatile effector cells in the normal and pathologic brain. Nat Neurosci, 10(11): 1387-94.

38 Paolicelli RC,Gross CT. (2011) Microglia in development: linking brain wiring to brain environment. Neuron Glia Biol, 7(1): 77-83.

39 Biber K, Neumann H, Inoue K,Boddeke HW. (2007) Neuronal 'On' and 'Off' signals control microglia. Trends Neurosci, 30(11): 596-602.

40 Ransohoff RM,Cardona AE. (2010) The myeloid cells of the central nervous system parenchyma. Nature, 468(7321): 253-62.

41 Saijo K,Glass CK. (2011) Microglial cell origin and phenotypes in health and disease. Nat Rev Immunol, 11(11): 775-87.

42 Patel AR, Ritzel R, McCullough LD,Liu F. (2013) Microglia and ischemic stroke: a double-edged sword. Int J Physiol Pathophysiol Pharmacol, 5(2): 73-90.

43 Habib P, Slowik A, Zendedel A, Johann S, Dang J,Beyer C. (2014) Regulation of hypoxia-induced inflammatory responses and M1-M2 phenotype switch of primary rat microglia by sex steroids. J Mol Neurosci, 52(2): 277-85.

44 Wang WY, Tan MS, Yu JT,Tan L. (2015) Role of pro-inflammatory cytokines released from microglia in Alzheimer's disease. Ann Transl Med, 3(10): 136.

45 Block ML, Zecca L,Hong JS. (2007) Microglia-mediated neurotoxicity: uncovering the molecular mechanisms. Nat Rev Neurosci, 8(1): 57-69.

46 Biber K, Vinet J,Boddeke HW. (2008) Neuron-microglia signaling: chemokines as versatile messengers. J Neuroimmunol, 198(1-2): 69-74.

47 Harrison JK, Jiang Y, Chen S, Xia Y, Maciejewski D, McNamara RK, Streit WJ, Salafranca MN, Adhikari S, Thompson DA, Botti P, Bacon KB,Feng L. (1998)

Role for neuronally derived fractalkine in mediating interactions between neurons and CX3CR1-expressing microglia. Proc Natl Acad Sci U S A, 95(18): 10896-901.

48 Cardona AE, Pioro EP, Sasse ME, Kostenko V, Cardona SM, Dijkstra IM, Huang D, Kidd G, Dombrowski S, Dutta R, Lee JC, Cook DN, Jung S, Lira SA, Littman DR,Ransohoff RM. (2006) Control of microglial neurotoxicity by the fractalkine receptor. Nat Neurosci, 9(7): 917-24.

49 Umehara H, Bloom ET, Okazaki T, Nagano Y, Yoshie O,Imai T. (2004) Fractalkine in vascular biology: from basic research to clinical disease. Arterioscler Thromb Vasc Biol, 24(1): 34-40.

50 Mizoue LS, Sullivan SK, King DS, Kledal TN, Schwartz TW, Bacon KB,Handel TM. (2001) Molecular determinants of receptor binding and signaling by the CX3C chemokine fractalkine. J Biol Chem, 276(36): 33906-14.

51 Lauro C, Catalano M, Trettel F,Limatola C. (2015) Fractalkine in the nervous system: neuroprotective or neurotoxic molecule? Ann N Y Acad Sci, 1351: 141-8.

52 Hundhausen C, Misztela D, Berkhout TA, Broadway N, Saftig P, Reiss K, Hartmann D, Fahrenholz F, Postina R, Matthews V, Kallen KJ, Rose-John S,Ludwig A. (2003) The disintegrin-like metalloproteinase ADAM10 is involved in constitutive cleavage of CX3CL1 (fractalkine) and regulates CX3CL1-mediated cell-cell adhesion. Blood, 102(4): 1186-95.

53 Garton KJ, Gough PJ, Blobel CP, Murphy G, Greaves DR, Dempsey PJ,Raines EW. (2001) Tumor necrosis factor-alpha-converting enzyme (ADAM17) mediates the cleavage and shedding of fractalkine (CX3CL1). J Biol Chem, 276(41): 37993-8001.

54 Bazan JF, Bacon KB, Hardiman G, Wang W, Soo K, Rossi D, Greaves DR, Zlotnik A,Schall TJ. (1997) A new class of membrane-bound chemokine with a CX3C motif. Nature, 385(6617): 640-4.

55 Kim KW, Vallon-Eberhard A, Zigmond E, Farache J, Shezen E, Shakhar G, Ludwig A, Lira SA,Jung S. (2011) In vivo structure/function and expression analysis of the CX3C chemokine fractalkine. Blood, 118(22): E156-E167.

56 Lucas AD, Chadwick N, Warren BF, Jewell DP, Gordon S, Powrie F,Greaves DR. (2001) The transmembrane form of the CX3CL1 chemokine fractalkine is expressed predominantly by epithelial cells in vivo. American Journal of Pathology, 158(3): 855-866.

57 Shah R, Hinkle CC, Ferguson JF, Mehta NN, Li M, Qu L, Lu Y, Putt ME, Ahima RS,Reilly MP. (2011) Fractalkine is a novel human adipochemokine associated with type 2 diabetes. Diabetes, 60(5): 1512-8.

58 Efsen E, Grappone C, DeFranco RM, Milani S, Romanelli RG, Bonacchi A, Caligiuri A, Failli P, Annunziato F, Pagliai G, Pinzani M, Laffi G, Gentilini P,Marra F. (2002) Up-regulated expression of fractalkine and its receptor CX3CR1 during liver injury in humans. J Hepatol, 37(1): 39-47.

59 Ludwig A, Berkhout T, Moores K, Groot P,Chapman G. (2002) Fractalkine is expressed by smooth muscle cells in response to IFN-gamma and TNF-alpha and is modulated by metalloproteinase activity. J Immunol, 168(2): 604-612.

60 Butoi ED, Gan AM, Manduteanu I, Stan D, Calin M, Pirvulescu M, Koenen RR, Weber C,Simionescu M. (2011) Cross talk between smooth muscle cells and monocytes/activated monocytes via CX3CL1/CX3CR1 axis augments expression of pro-atherogenic molecules. Biochim Biophys Acta, 1813(12): 2026-2035.

61 Yoshida H, Imaizumi T, Fujimoto K, Matsuo N, Kimura K, Cui X, Matsumiya T, Tanji K, Shibata T, Tamo W, Kumagai M,Satoh K. (2001) Synergistic stimulation, by tumor necrosis factor-alpha and interferon-gamma, of fractalkine expression in human astrocytes. Neurosci Lett, 303(2): 132-6.

62 Imai T, Hieshima K, Haskell C, Baba M, Nagira M, Nishimura M, Kakizaki M, Takagi S, Nomiyama H, Schall TJ,Yoshie O. (1997) Identification and molecular characterization of fractalkine receptor CX3CR1, which mediates both leukocyte migration and adhesion. Cell, 91(4): 521-30.

63 Nishiyori A, Minami M, Ohtani Y, Takami S, Yamamoto J, Kawaguchi N, Kume T, Akaike A,Satoh M. (1998) Localization of fractalkine and CX3CR1 mRNAs in rat brain: does fractalkine play a role in signaling from neuron to microglia? FEBS Lett, 429(2): 167-72.

64 Jung S, Aliberti J, Graemmel P, Sunshine MJ, Kreutzberg GW, Sher A,Littman DR. (2000) Analysis of fractalkine receptor CX(3)CR1 function by targeted deletion and green fluorescent protein reporter gene insertion. Mol Cell Biol, 20(11): 4106-14.

65 Zhan Y, Paolicelli RC, Sforazzini F, Weinhard L, Bolasco G, Pagani F, Vyssotski AL, Bifone A, Gozzi A, Ragozzino D,Gross CT. (2014) Deficient neuron-

microglia signaling results in impaired functional brain connectivity and social behavior. Nat Neurosci, 17(3): 400-6.

66 Yirmiya R, Rimmerman N,Reshef R. (2015) Depression as a microglial disease. Trends Neurosci, 38(10): 637-58.

67 Corona AW, Huang Y, O'Connor JC, Dantzer R, Kelley KW, Popovich PG,Godbout JP. (2010) Fractalkine receptor (CX3CR1) deficiency sensitizes mice to the behavioral changes induced by lipopolysaccharide. J Neuroinflammation, 7: 93.

68 Horai R, Asano M, Sudo K, Kanuka H, Suzuki M, Nishihara M, Takahashi M,Iwakura Y. (1998) Production of mice deficient in genes for interleukin (IL)-1alpha, IL-1beta, IL-1alpha/beta, and IL-1 receptor antagonist shows that IL-1beta is crucial in turpentine-induced fever development and glucocorticoid secretion. J Exp Med, 187(9): 1463-75.

69 Fuchsl AM, Neumann ID,Reber SO. (2014) Stress resilience: a low-anxiety genotype protects male mice from the consequences of chronic psychosocial stress. Endocrinology, 155(1): 117-26.

70 Veenema AH, Bredewold R,Neumann ID. (2007) Opposite effects of maternal separation on intermale and maternal aggression in C57BL/6 mice: link to hypothalamic vasopressin and oxytocin immunoreactivity. Psychoneuroendocrinology, 32(5): 437-50.

71 Herman JP, Adams D,Prewitt C. (1995) Regulatory changes in neuroendocrine stress-integrative circuitry produced by a variable stress paradigm. Neuroendocrinology, 61(2): 180-90.

72 Tremblay ME, Zettel ML, Ison JR, Allen PD,Majewska AK. (2012) Effects of aging and sensory loss on glial cells in mouse visual and auditory cortices. Glia, 60(4): 541-58.

73 Simmons DM, Arriza, J.L., Swanson, L.W.,. (1989.) A complete protocol for in situ hybridization of messenger RNAs in brain and other tissues with radiolabeled single-stranded RNA probes. J. Histotechnol., (12): 169–181.

74 Kovacs KJ,Makara GB. (1988) Corticosterone and dexamethasone act at different brain sites to inhibit adrenalectomy-induced adrenocorticotropin hypersecretion. Brain Res, 474(2): 205-10.

75 Zelena D, Mergl Z, Foldes A, Kovacs KJ, Toth Z,Makara GB. (2003) Role of hypothalamic inputs in maintaining pituitary-adrenal responsiveness in repeated restraint. Am J Physiol Endocrinol Metab, 285(5): E1110-7.

76 Winkler Z, Kuti D, Ferenczi S, Gulyas K, Polyak A,Kovacs KJ. (2017) Impaired microglia fractalkine signaling affects stress reaction and coping style in mice. Behav Brain Res, 334: 119-128.

77 Cook CJ. (2004) Stress induces CRF release in the paraventricular nucleus, and both CRF and GABA release in the amygdala. Physiol Behav, 82(4): 751-62.

78 Veenema AH, Reber SO, Selch S, Obermeier F,Neumann ID. (2008) Early life stress enhances the vulnerability to chronic psychosocial stress and experimental colitis in adult mice. Endocrinology, 149(6): 2727-36.

79 Ferenczi S, Zelei E, Pinter B, Szoke Z,Kovacs KJ. (2010) Differential regulation of hypothalamic neuropeptide Y hnRNA and mRNA during psychological stress and insulin-induced hypoglycemia. Mol Cell Endocrinol, 321(2): 138-45.

80 Polyak A, Winkler Z, Kuti D, Ferenczi S,Kovacs KJ. (2016) Brown adipose tissue in obesity: Fractalkine-receptor dependent immune cell recruitment affects metabolic-related gene expression. Biochim Biophys Acta, 1861(11): 1614-1622.

81 Schubert I, Ahlbrand R, Winter A, Vollmer L, Lewkowich I,Sah R. (2017) Enhanced fear and altered neuronal activation in forebrain limbic regions of CX3CR1-deficient mice. Brain Behav Immun, 68:34-43.

82 Koolhaas JM, Korte SM, De Boer SF, Van Der Vegt BJ, Van Reenen CG, Hopster H, De Jong IC, Ruis MA,Blokhuis HJ. (1999) Coping styles in animals: current status in behavior and stress-physiology. Neurosci Biobehav Rev, 23(7): 925-35.

83 Hellwig S, Brioschi S, Dieni S, Frings L, Masuch A, Blank T,Biber K. (2016) Altered microglia morphology and higher resilience to stress-induced depression-like behavior in CX3CR1-deficient mice. Brain Behav Immun, 55: 126-37.

84 Milior G, Lecours C, Samson L, Bisht K, Poggini S, Pagani F, Deflorio C, Lauro C, Alboni S, Limatola C, Branchi I, Tremblay ME,Maggi L. (2016) Fractalkine receptor deficiency impairs microglial and neuronal responsiveness to chronic stress. Brain Behav Immun, 55: 114-25.

85 Chen X,Herbert J. (1995) Regional changes in c-fos expression in the basal forebrain and brainstem during adaptation to repeated stress: correlations with cardiovascular, hypothermic and endocrine responses. Neuroscience, 64(3): 675-85.

86 Mezey E, Reisine TD, Brownstein MJ, Palkovits M,Axelrod J. (1984) Beta-adrenergic mechanism of insulin-induced adrenocorticotropin release from the anterior pituitary. Science, 226(4678): 1085-7.

87 Melia KR, Ryabinin AE, Schroeder R, Bloom FE,Wilson MC. (1994) Induction and habituation of immediate early gene expression in rat brain by acute and repeated restraint stress. J Neurosci, 14(10): 5929-38.

88 Brown ER,Sawchenko PE. (1997) Hypophysiotropic CRF neurons display a sustained immediate-early gene response to chronic stress but not to adrenalectomy. J Neuroendocrinol, 9(4): 307-16.

89 O'Mahony CM, Sweeney FF, Daly E, Dinan TG,Cryan JF. (2010) Restraint stress-induced brain activation patterns in two strains of mice differing in their anxiety behaviour. Behav Brain Res, 213(2): 148-54.

90 Aguilera G,Liu Y. (2012) The molecular physiology of CRH neurons. Front Neuroendocrinol, 33(1): 67-84.

91 Herman JP, Ostrander MM, Mueller NK,Figueiredo H. (2005) Limbic system mechanisms of stress regulation: hypothalamo-pituitary-adrenocortical axis. Prog Neuropsychopharmacol Biol Psychiatry, 29(8): 1201-13.

92 Paolicelli RC, Bolasco G, Pagani F, Maggi L, Scianni M, Panzanelli P, Giustetto M, Ferreira TA, Guiducci E, Dumas L, Ragozzino D,Gross CT. (2011) Synaptic pruning by microglia is necessary for normal brain development. Science, 333(6048): 1456-8.

93 McNeilly AD, Stewart CA, Sutherland C,Balfour DJ. (2015) High fat feeding is associated with stimulation of the hypothalamic-pituitary-adrenal axis and reduced anxiety in the rat. Psychoneuroendocrinology, 52: 272-80.

94 Polyák Á, Ferenczi S, Dénes Á, Winkler Z, Kriszt R, Pintér-Kübler B,Kovács KJ. (2014) The fractalkine/Cx3CR1 system is implicated in the development of metabolic visceral adipose tissue inflammation in obesity. Brain Behav Immun, 38(0): 25-35.

95 Fleshner M, Frank M,Maier SF. (2017) Danger Signals and Inflammasomes: Stress-Evoked Sterile Inflammation in Mood Disorders. Neuropsychopharmacology, 42(1): 36-45.

96 Frank MG, Weber MD, Watkins LR,Maier SF. (2015) Stress sounds the alarmin: The role of the danger-associated molecular pattern HMGB1 in stress-induced neuroinflammatory priming. Brain Behav Immun, 48:1-7.

97 Fleshner M. (2013) Stress-evoked sterile inflammation, danger associated molecular patterns (DAMPs), microbial associated molecular patterns (MAMPs) and the inflammasome. Brain Behav Immun, 27(1): 1-7.

98 Maslanik T, Mahaffey L, Tannura K, Beninson L, Greenwood BN,Fleshner M. (2013) The inflammasome and danger associated molecular patterns (DAMPs) are implicated in cytokine and chemokine responses following stressor exposure. Brain Behav Immun, 28: 54-62.

99 Miller RE, Belmadani A, Ishihara S, Tran PB, Ren D, Miller RJ,Malfait AM. (2015) Damage-associated molecular patterns generated in osteoarthritis directly excite murine nociceptive neurons through Toll-like receptor 4. Arthritis Rheumatol, 67(11): 2933-43.

100 Weber MD, Frank MG, Tracey KJ, Watkins LR,Maier SF. (2015) Stress induces the danger-associated molecular pattern HMGB-1 in the hippocampus of male Sprague Dawley rats: a priming stimulus of microglia and the NLRP3 inflammasome. J Neurosci, 35(1): 316-24.

101 Hinwood M, Morandini J, Day TA,Walker FR. (2012) Evidence that microglia mediate the neurobiological effects of chronic psychological stress on the medial prefrontal cortex. Cereb Cortex, 22(6): 1442-54.

102 Sugama S, Fujita M, Hashimoto M,Conti B. (2007) Stress induced morphological microglial activation in the rodent brain: involvement of interleukin-18. Neuroscience, 146(3): 1388-99.

103 Tynan RJ, Naicker S, Hinwood M, Nalivaiko E, Buller KM, Pow DV, Day TA,Walker FR. (2010) Chronic stress alters the density and morphology of microglia in a subset of stress-responsive brain regions. Brain Behav Immun, 24(7): 1058-68.

104 Kopp BL, Wick D,Herman JP. (2013) Differential effects of homotypic vs. heterotypic chronic stress regimens on microglial activation in the prefrontal cortex. Physiol Behav, 122: 246-52.

105 Sugama S, Takenouchi T, Fujita M, Kitani H, Conti B,Hashimoto M. (2013) Corticosteroids limit microglial activation occurring during acute stress. Neuroscience, 232: 13-20.

106 Ham M, Choe SS, Shin KC, Choi G, Kim JW, Noh JR, Kim YH, Ryu JW, Yoon KH, Lee CH,Kim JB. (2016) Glucose-6-Phosphate Dehydrogenase Deficiency Improves Insulin Resistance With Reduced Adipose Tissue Inflammation in Obesity. Diabetes, 65(9): 2624-38.

107 Gregor MF,Hotamisligil GS. (2011) Inflammatory mechanisms in obesity. Annu Rev Immunol, 29: 415-45.

108 Thaler JP, Yi CX, Schur EA, Guyenet SJ, Hwang BH, Dietrich MO, Zhao X, Sarruf DA, Izgur V, Maravilla KR, Nguyen HT, Fischer JD, Matsen ME, Wisse BE, Morton GJ, Horvath TL, Baskin DG, Tschop MH,Schwartz MW. (2012) Obesity is associated with hypothalamic injury in rodents and humans. J Clin Invest, 122(1): 153-62.

109 Freire-Regatillo A, Argente-Arizon P, Argente J, Garcia-Segura LM,Chowen JA. (2017) Non-Neuronal Cells in the Hypothalamic Adaptation to Metabolic Signals. Front Endocrinol (Lausanne), 8: 51.

110 Valdearcos M, Douglass JD, Robblee MM, Dorfman MD, Stifler DR, Bennett ML, Gerritse I, Fasnacht R, Barres BA, Thaler JP,Koliwad SK. (2017) Microglial Inflammatory Signaling Orchestrates the Hypothalamic Immune Response to Dietary Excess and Mediates Obesity Susceptibility. Cell Metab, 26(1): 185-197.e3.

111 Morari J, Anhe GF, Nascimento LF, de Moura RF, Razolli D, Solon C, Guadagnini D, Souza G, Mattos AH, Tobar N, Ramos CD, Pascoal VD, Saad MJ, Lopes-Cendes I, Moraes JC,Velloso LA. (2014) Fractalkine (CX3CL1) is involved in the early activation of hypothalamic inflammation in experimental obesity. Diabetes, 63(11): 3770-84.

112 Kettenmann H, Hanisch UK, Noda M,Verkhratsky A. (2011) Physiology of microglia. Physiol Rev, 91(2): 461-553.

113 Ramonet D, Rodriguez MJ, Pugliese M,Mahy N. (2004) Putative glucosensing property in rat and human activated microglia. Neurobiol Dis, 17(1): 1-9.

114 Kurita H, Xu KY, Maejima Y, Nakata M, Dezaki K, Santoso P, Yang Y, Arai T, Gantulga D, Muroya S, Lefor AK, Kakei M, Watanabe E,Yada T. (2015) Arcuate Na+,K+-ATPase senses systemic energy states and regulates feeding behavior through glucose-inhibited neurons. Am J Physiol Endocrinol Metab, 309(4): E320-33.

115 Melani A, Turchi D, Vannucchi MG, Cipriani S, Gianfriddo M,Pedata F. (2005) ATP extracellular concentrations are increased in the rat striatum during in vivo ischemia. Neurochem Int, 47(6): 442-8.

116 Ferrari D, Chiozzi P, Falzoni S, Hanau S,Di Virgilio F. (1997) Purinergic modulation of interleukin-1 beta release from microglial cells stimulated with bacterial endotoxin. J Exp Med, 185(3): 579-82.

117 Yrjanheikki J, Keinanen R, Pellikka M, Hokfelt T,Koistinaho J. (1998) Tetracyclines inhibit microglial activation and are neuroprotective in global brain ischemia. Proc Natl Acad Sci U S A, 95(26): 15769-74.

118 Dinarello CA. (1997) Interleukin-1. Cytokine Growth Factor Rev, 8(4): 253-65.

119 Hajmrle C, Smith N, Spigelman AF, Dai X, Senior L, Bautista A, Ferdaoussi M,MacDonald PE. (2016) Interleukin-1 signaling contributes to acute islet compensation. JCI Insight, 1(4): e86055.

120 Spulber S, Mateos L, Oprica M, Cedazo-Minguez A, Bartfai T, Winblad B,Schultzberg M. (2009) Impaired long term memory consolidation in transgenic mice overexpressing the human soluble form of IL-1ra in the brain. J Neuroimmunol, 208(1-2): 46-53.

121 Minami M, Kuraishi Y, Yamaguchi T, Nakai S, Hirai Y,Satoh M. (1991) Immobilization stress induces interleukin-1 beta mRNA in the rat hypothalamus. Neurosci Lett, 123(2): 254-6.

122 Ericsson A, Kovacs KJ,Sawchenko PE. (1994) A functional anatomical analysis of central pathways subserving the effects of interleukin-1 on stress-related neuroendocrine neurons. J Neurosci, 14(2): 897-913.

123 Del Rey A, Verdenhalven M, Lorwald AC, Meyer C, Hernangomez M, Randolf A, Roggero E, Konig AM, Heverhagen JT, Guaza C,Besedovsky HO. (2016) Brain-

borne IL-1 adjusts glucoregulation and provides fuel support to astrocytes and neurons in an autocrine/paracrine manner. Mol Psychiatry, 21(9): 1309-20.

124 Spielman LJ, Bahniwal M, Little JP, Walker DG,Klegeris A. (2015) Insulin Modulates In Vitro Secretion of Cytokines and Cytotoxins by Human Glial Cells. Curr Alzheimer Res, 12(7): 684-93.

125 Oguri S, Motegi K, Iwakura Y,Endo Y. (2002) Primary role of interleukin-1 alpha and interleukin-1 beta in lipopolysaccharide-induced hypoglycemia in mice. Clin Diagn Lab Immunol, 9(6): 1307-12.

126 Del Rey A,Besedovsky HO. (1992) Metabolic and neuroendocrine effects of pro-inflammatory cytokines. Eur J Clin Invest, 22 Suppl 1: 10-5.

127 Segel SA, Paramore DS,Cryer PE. (2002) Hypoglycemia-associated autonomic failure in advanced type 2 diabetes. Diabetes, 51(3): 724-33.

DOI:10.14753/SE.2018.2148

11. Bibliography of the candidate's publications

Publications that form the basis of the Ph.D. dissertation:

Winkler Z, Kuti D, Ferenczi S, Gulyas K, Polyak A, Kovacs KJ. (2017) Impaired microglia fractalkine signaling affects stress reaction and coping style in mice. Behav Brain Res, 334: 119-128.

Polyak A, Winkler Z, Kuti D, Ferenczi S, Kovacs KJ. (2016) Brown adipose tissue in obesity: Fractalkine-receptor dependent immune cell recruitment affects metabolic-related gene expression. Biochim Biophys Acta, 1861: 1614-1622.

Polyak A, Ferenczi S, Denes A, Winkler Z, Kriszt R, Pinter-Kubler B, Kovacs KJ. (2014) The fractalkine/Cx3CR1 system is implicated in the development of metabolic visceral adipose tissue inflammation in obesity. Brain Behav Immun, 38: 25-35.

Other publications

Ferenczi S, Szegi K, Winkler Z, Barna T, Kovacs KJ. (2016) Oligomannan Prebiotic Attenuates Immunological, Clinical and Behavioral Symptoms in Mouse Model of Inflammatory Bowel Disease. Sci Rep, 6: 34132.

Kriszt R, Winkler Z, Polyak A, Kuti D, Molnar C, Hrabovszky E, Kallo I, Szoke Z, Ferenczi S, Kovacs KJ. (2015) Xenoestrogens Ethinyl Estradiol and Zearalenone Cause Precocious Puberty in Female Rats via Central Kisspeptin Signaling. Endocrinology, 156:3996-4007.

DOI:10.14753/SE.2018.2148

12. Acknowledgements

First and foremost, I would like to thank my supervisor Krisztina Kovács for guiding and supporting me over the years, and that she promoted my scientific progress from the beginning of my studies.

I am grateful to my all the past and present colleagues of the Laboratory of Molecular Neuroendocrinology: Julianna Benkő, Szilamér Ferenczi, Krisztina Gulyás, Krisztina Horváth, Dóra Kővári, Dániel Kuti, Bernadett Küblerné Pintér, Rókus Kriszt and Ágnes Polyák for their help.

I wish to thank to co-workers at Institute of Experimental Medicine, particularly to Ádám Dénes, Nikolett Lénárt, Csaba Fekete for their help to extend my technical background.

Last, but not least, I would like to express my thanks to my family and friends for their encouragement during my studies and the preparation of my PhD dissertation.